Inorganic Chemistry

ARTICLE

pubs.acs.org/IC

Synthesis and Structure of Ruthenium(IV) Complexes Featuring N-Heterocyclic Ligands with an N−H Group as the Hydrogen-Bond Donor: Hydrogen Interactions in Solution and in the Solid State

Josefina Díez,[†] José Gimeno,[*,†] Isabel Merino,[‡] Eduardo Rubio,[*,†,‡] and Francisco J. Suárez[†]

[†]Departamento de Química Orgánica e Inorgánica, Instituto Universitario de Química Organometálica "Enrique Moles" (Unidad Asociada al CSIC), Universidad de Oviedo, 33071 Oviedo, Spain

[‡]Unidad de Resonancia Magnética Nuclear, Servicios Científico-Técnicos de la Universidad de Oviedo, 33071 Oviedo, Spain

Supporting Information

ABSTRACT: The synthesis and characterization of novel ruthenium(IV) complexes $[Ru(\eta^3:\eta^3\text{-}C_{10}H_{16})Cl_2L]$ [L = 3-methylpyrazole (**2b**), 3,5-dimethylpyrazole (**2c**), 3-methyl-5-phenylpyrazole (**2d**), 2-(1*H*-pyrazol-5-yl)phenol (**2e**), 6-azauracile (**3**), and 1*H*-indazol-3-ol (**4**)] are reported. Complex **2e** is converted to the chelated complex $[Ru(\eta^3:\eta^3\text{-}C_{10}H_{16})Cl(\kappa^2\text{-}N,O\text{-}2\text{-}(1H\text{-pyrazol-3-yl})\text{phenoxy})]$ (**5**) by treatment with an excess of NaOH. All of the ligands feature N−H, O−H, or C═O as the potential hydrogen-bonding group. The structures of complexes **2a**−**2c**, **2e**, **3**, and **5** in the solid state have been determined by X-ray diffraction. Complexes **2a**−**2c** and **3**, which contain the pyrazole N−H group, exhibit intra- and intermolecular hydrogen bonds with chloride ligands [N−H···Cl distances (Å): intramolecular, 2.30−2.78; intermolecular, 2.59−2.77]. Complexes **2e** and **3** bearing respectively O−H and C═O groups also feature N−H···O interactions [intramolecular (**2e**), 2.27 Å; intermolecular (**3**), 2.00 Å]. Chelated complex **5**, lacking the O−H group, only shows an intramolecular N−H···Cl hydrogen bonding of 2.42 Å. The structure of complex **3**, which turns out to be a dimer in the solid state through a double intermolecular N−H···O hydrogen bonding, has also been investigated in solution (CD_2Cl_2) by NMR diffusion studies. Diffusion-ordered spectroscopy experiments reveal an equilibrium between monomer and dimer species in solution whose extension depends on the temperature, concentration, and coordinating properties of the solvent. Preliminary catalytic studies show that complex **3** is highly active in the redox isomerization of the allylic alcohols in an aqueous medium under very mild reaction conditions (35 °C) and in the absence of a base.

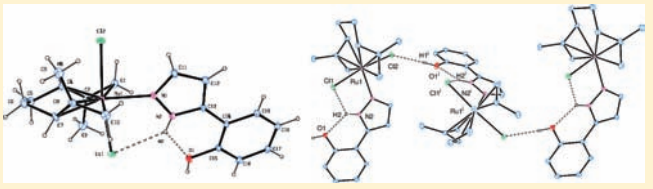

INTRODUCTION

Since the first reports on the existence of the hydrogen bond around a century ago, there has been a growing interest in this type of interaction, which plays a key role in numerous chemical systems ranging from inorganic and organic to biological chemistry.[1] The abilities of proteins to fold into stable three-dimensional structures and to link small and large molecules such as the double-helical structures of DNA and RNA macromolecules are among the most important manifestations. Hydrogen bonding is also responsible for the remarkable selectivity and acceleration rate observed in ubiquitous enzymatic processes of biological interest. On the other hand, its utilization as an activation force has become a powerful tool in modern organocatalysis.[2]

Metalloenzymes, which combine the properties of metals and hydrogen bonds, are also very common natural catalysts of important biological processes whose active sites generally exhibit many hydrogen interactions.[3] Because natural processes exploit these properties to accomplish very important chemical transformations, the design of metal complexes bearing hydrogen-bonding groups for a practical use is a goal of current special interest. In this regard, new types of these interactions have emerged as crucial structural and functional features in metal complexes, providing relevant examples with unusual properties in several fields.[4] The development of new materials and complexes that behave as sensors, chromophores, and medicines, among other applications, has recently been described.[5]

In order to mimic the metalloenzyme activity in natural systems, there has been a growing interest to enhance the metal catalysts and substrate binding via the promotion of hydrogen bonding. The key point of this favorable catalytic activity stems from the cooperative effects provided by the bifunctional character of molecular catalysts, which may act as both acidic and basic active sites in metalloenzymes.[6] The most genuine catalytic transformations of this type, in terms of high selectivity and rate enhancement, are concerned with transition states characterized by "outer-sphere" hydrogen bonding featuring low-energy barriers responsible for high catalytic performances and enantioselectivities (Figure 1).[7] Typical examples showing this type of interaction[8,9] are involved in the hydrogenation of polar functional groups such as aldehydes, ketones, or imines catalyzed by semisandwich ruthenium(II) hydrides [Noyori's (**A**)[7a] and

Received: January 18, 2011
Published: May 10, 2011

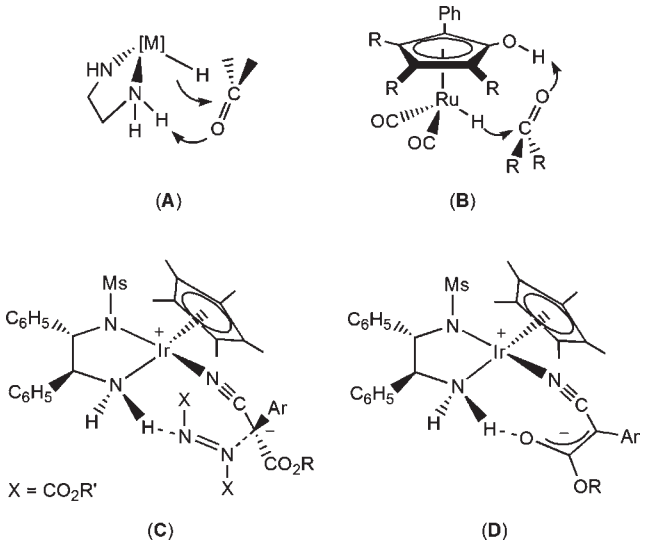

Figure 1. Examples of catalytic species featuring "outer-sphere" hydrogen bonding.

Chart 1

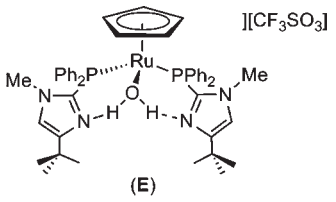

Shvo's (**B**)[7b−d] catalysts] as well as iridium(III) complexes (**C** and **D**) proposed in the catalyzed asymmetric C−C and C−N bond formation.[7l]

Water often plays a prominent role in the active sites of metalloenzymes via the formation of weak noncovalent hydrogen bonding. However, examples in which these interactions enhance the catalytic activity of transition-metal complexes in aqueous media have remained elusive. Recently, ruthenium-catalyzed regioselective and highly efficient procedures in the hydration of alkynes[10] and nitriles[11] to give aldehydes and amides, respectively, have been reported.[12] Significantly, an intermediate aquaruthenium(II) complex displaying an intramolecular N···H hydrogen bonding of pendant κ-P bidentate *P,N*-imidazolylphosphane ligands with water has been isolated (**E**, Chart 1).[10b] This fact is assumed to be responsible for the observed high catalytic efficiency.

With these precedents in mind and in the context of our ongoing interest in the study of ruthenium-catalyzed reactions, we have devoted special attention to efficient catalytic transformations in aqueous media.[13] In this regard, we are engaged in the synthesis of new active catalysts with structural features enabling hydrogen interactions to be used as potential bifunctional catalysts in aqueous media. Herein, we describe the synthesis and characterization of new ruthenium(IV) complexes bearing N-heterocyclic ligands functionalized with uncoordinated C═O, N−H, and O−H groups (**F**−**I**, Chart 2), which are prone to form hydrogen bonds. Molecular structures determined by X-ray diffraction studies showing unequivocal information on inter- and intramolecular hydrogen bonding in the solid state are reported. The results of NMR studies using variable-temperature and diffusion-ordered spectroscopy (DOSY) experiments for a model complex show that these interactions also exist in solution. Preliminary catalytic studies on the redox isomerization of allylic alcohols in water using the uracile derivative **I** as a catalyst are also described, revealing a high activity under very mild reaction conditions (35 °C) and in the absence of a base.

Chart 2

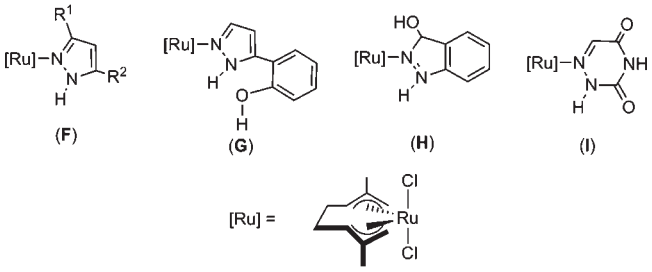

EXPERIMENTAL SECTION

The manipulations were performed under an atmosphere of dry nitrogen using vacuum-line and standard Schlenk techniques. Solvents were dried by standard methods and distilled under nitrogen before use. All reagents were obtained from commercial suppliers and used without further purification with the exception of compounds $[\{Ru(\eta^3:\eta^3\text{-}C_{10}H_{16})(\mu\text{-}Cl)Cl\}_2]$ (**1**)[14] and $[Ru(\eta^3:\eta^3\text{-}C_{10}H_{16})Cl_2(pyrazole)]$ (**2a**),[15] which were prepared by following the methods reported in the literature. IR spectra were recorded on a Perkin-Elmer 1720-XFT spectrometer. The conductivities were measured at room temperature, in ca. 10^{-3} mol dm^{-3} water solutions, with a Jenway PCM3 conductimeter. C, H, and N analyses were carried out with a Perkin-Elmer 2400 microanalyzer. NMR spectra were recorded on a Bruker DPX-300 instrument at 300 MHz (^{1}H) or 75.4 MHz (^{13}C) using $SiMe_4$ as the standard. DEPT experiments have been carried out for all of the compounds reported. The numbering for the protons and carbons of the 2,7-dimethylocta-2,6-diene-1,8-diyl skeleton is as follows:

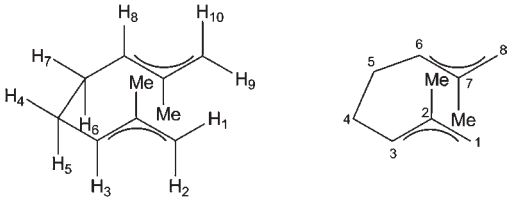

Synthesis of Complexes $[Ru(\eta^3:\eta^3\text{-}C_{10}H_{16})Cl_2L]$ [L = 3-Methylpyrazole (2b), 3,5-Dimethylpyrazole (2c), 3-Methyl-5-phenylpyrazole (2d), 2-(1*H*-Pyrazol-3-yl)phenol (2e), 6-Azauracil (3), and 2-Indazolinone (4)]. The corresponding ligand (0.64 mmol) was added, at room temperature, to a solution of complex **1** (0.200 g; 0.32 mmol) in 20 mL of dichloromethane. After the mixture was stirred for 10 min, the solvent was removed under vacuum and the resulting orange solid residue was washed with hexane (3 × 10 mL) and dried in vacuo. **2b**. Yield: 76% (191 mg). Anal. Calcd for $RuC_{14}H_{22}Cl_2N_2$: C, 43.08; H, 5.68; N, 7.18. Found: C, 42.91; H, 5.59; N, 7.15. IR (KBr, cm^{-1}): ν 605 (m), 684 (s), 781 (mf), 952 (m), 1109 (s), 1282 (s), 1385 (s), 1463 (m), 1563 (m), 2913 (m), 3281 (s). ^{1}H NMR (CD_2Cl_2): δ 2.37 (s, 6H, CH_3), 2.40 (s, 3H, CH_3 L), 2.47 (m, 2H, H_4 and H_6), 3.09 (m, 2H, H_5 and H_7), 4.34 (s, 2H, H_2 and H_{10}), 4.48 (s,

dx.doi.org/10.1021/ic200547k |*Inorg. Chem.* 2011, 50, 4868–4881

2H, H_1 and H_9), 5.18 (m, 2H, H_3 and H_8), 6.27 (s, 1H, H_4 L), 8.16 (s, 1H, H_3 L), 11.74 (s, 1H, NH). $^{13}C\{^1H\}$ NMR (CD_2Cl_2): δ 11.0 (s, CH_3), 20.9 (s, CH_3), 36.7 (s, C_4 and C_5), 76.9 (s, C_1 and C_8), 94.5 (s, C_3 and C_6), 106.8 (s, C_4 L), 130.0 (s, C_2 and C_7), 141.8 (s, C_5 L), 143.2 (s, C_3 L). **2c**. Yield: 57% (148 mg). Anal. Calcd for $RuC_{15}H_{24}Cl_2N_2$: C, 44.56; H, 5.98; N, 6.93. Found: C, 45.05; H, 5.86; N, 7.00. IR (KBr, cm^{-1}): ν 660 (m), 803 (s), 955 (m), 1021 (s), 1149 (m), 1283 (s), 1390 (m), 1570 (vs), 2907 (m), 3312 (s). ^1H NMR (CD_2Cl_2): δ 2.26 (s, 3H, CH_3 in C_3 L), 2.35 (m, 2H, H_4 and H_6), 2.37 (s, 6H, CH_3), 2.43 (s, 3H, CH_3 in C_5 L), 3.00 (m, 2H, H_5 and H_7), 4.49 (s, 2H, H_2 and H_{10}), 4.88 (s, 2H, H_1 and H_9), 5.15 (m, 2H, H_3 and H_8), 5.95 (s, 1H, H_4 L), 11.21 (s, 1H, NH). $^{13}C\{^1H\}$ NMR (CD_2Cl_2): δ 10.7 (s, CH_3 in C_3 L), 15.7 (s, CH_3 in C_5 L), 20.9 (s, $2CH_3$), 36.3 (s, C_4 and C_5), 76.5 (s, C_1 and C_8), 95.0 (s, C_3 and C_6), 108.7 (s, C_4 L), 130.7 (s, C_2 and C_7), 141.4 (s, C_5 L), 157.9 (s, C_3 L). **2d**. Yield: 86% (260 mg). Anal. Calcd for $RuC_{20}H_{26}Cl_2N_2$: C, 51.50; H, 5.62; N, 6.01. Found: C, 51.43; H, 5.88; N, 6.04. IR (KBr, cm^{-1}): ν 693 (s), 763 (vs), 1022 (vs), 1294 (s), 1382 (s), 1467 (s), 1496 (s), 1564 (m), 2909 (m), 3222 (s). ^1H (CD_2Cl_2): δ 2.35 (m, 2H, H_4 and H_6), 2.40 (s, 6H, $2CH_3$), 2.61 (s, 3H, CH_3 in C_3 L), 3.02 (m, 2H, H_5 and H_7), 4.59 (s, 2H, H_2 and H_{10}), 4.93 (s, 2H, H_1 and H_9), 5.21 (m, 2H, H_3 and H_8), 6.45 (s, 1H, H_4 L), 7.35−7.52 (m, 5H, Ph), 12.04 (s, 1H, NH). $^{13}C\{^1H\}$ NMR (CD_2Cl_2): δ 15.8 (s, CH_3 in C_3 L), 21.1 (s, $2CH_3$), 36.4 (s, C_4 and C_5), 76.5 (s, C_1 and C_8), 95.1 (s, C_3 and C_6), 106.6 (s, C_4 L), 125.3 (s, C_o Ph), 128.3 (s, C_{ipso} Ph), 129.1 (s, C_p Ph), 129.2 (s, C_m Ph), 131.2 (s, C_2 and C_7), 144.3 (s, C_5 L), 158.8 (s, C_3 L). **2e**. Yield: 60% (180 mg). Anal. Calcd for $RuC_{19}H_{24}Cl_2N_2O$: C, 48.72; H, 5.16; N, 5.98. Found: C, 48.51; H, 5.70; N, 5.9. IR (KBr, cm^{-1}): ν 743 (vs), 779 (s), 957 (s), 1083 (vs), 1116 (s), 1243 (s), 1258 (s), 1345 (m), 1383 (m), 1444 (s), 1490 (s), 1552 (m), 1594 (m), 1612 (m), 2973 (m), 3202 (s). ^1H NMR (CD_2Cl_2): δ 2.33 (s, 6H, $2CH_3$), 2.43 (m, 2H, H_4 and H_6), 3.08 (m, 2H, H_5 and H_7), 4.35 (s, 2H, H_2 and H_{10}), 4.50 (s, 2H, H_1 and H_9), 5.17 (m, 2H, H_3 and H_8), 5.97 (s, 1H, OH), 6.82 (s, 1H, H_4 L), 6.90 (d, J_{HH} = 8.1 Hz, 1H, H_6 Ph), 7.03 (t, J_{HH} = 7.5 Hz, 1H, H_4 Ph), 7.23 (t, J_{HH} = 7.8 Hz, 1H, H_5 Ph), 7.65 (d, J_{HH} = 7.6 Hz, 1H, H_3 Ph), 7.27 (s, 1H, H_3 L), 12.85 (s, 1H, NH). $^{13}C\{^1H\}$ NMR (CD_2Cl_2): δ 21.0 (s, $2CH_3$), 36.7 (s, C_4 and C_5), 77.0 (s, C_1 and C_8), 94.7 (s, C_3 and C_6), 104.3 (s, C_4 L), 115.3 (s, C_2 Ph), 116.6 (s, C_6 Ph), 121.4 (s, C_4 Ph), 127.6 (s, C_3 Ph), 130.2 (s, C_5 Ph), 129.9 (s, C_2 and C_7), 142.5 (s, C_3 L), 142.7 (s, C_5 L), 152.3 (s, C_1 Ph).

3. Yield: 76% (204 mg). Anal. Calcd for $RuC_{13}H_{19}Cl_2N_3O_2$: C, 37.06; H, 4.55; N, 9.97. Found: C, 37.16; H, 4.45; N, 9.92. IR (KBr, cm^{-1}): ν 570 (s), 787 (m), 857 (m), 1021 (m), 1108 (m), 1383 (m), 1444 (s), 1609 (m), 1685 (vs), 1726 (vs), 3086 (s), 3430 (s). ^1H NMR (CD_2Cl_2): δ 2.41 (s, 6H, $2CH_3$), 2.43 (m, 2H, H_4 and H_6), 3.09 (m, 2H, H_5 and H_7), 4.35 (s, 2H, H_2 and H_{10}), 4.86 (s, 2H, H_1 and H_9), 5.36 (m, 2H, H_3 and H_8), 8.65 (s, 1H, CH, L), 9.10 and 11.74 (s, 2NH). $^{13}C\{^1H\}$ NMR (CD_2Cl_2): δ 21.0 (s, $2CH_3$), 36.3 (s, C_4 and C_5), 77.5 (s, C_1 and C_8), 95.0 (s, C_3 and C_6), 133.4 (s, C_2 and C_7), 143.1 (s, C_5 L), 146.5 (s, C_4 L), 154.3 (s, C_2 L). Conductivity (water, 20 °C): 177 Ω^{-1} cm^2 mol^{-1}.

4. Yield: 43% (122 mg). Anal. Calcd for $RuC_{17}H_{22}Cl_2N_2O$: C, 46.16; H, 5.01; N, 6.33. Found: C, 46.80; H, 4.93; N, 6.25. IR (KBr, cm^{-1}): ν 633 (m), 745 (s), 950 (m), 1352 (m), 1624 (s), 3295 (vs), 3446 (vs). ^1H NMR (CD_2Cl_2): δ 2.39 (s, 6H, $2CH_3$), 2.45 (m, 2H, H_4 and H_6), 3.10 (m, 2H, H_5 and H_7), 4.35 and 4.66 (s, 2H, H_2 and H_{10}), 4.90 and 5.27 (s, 2H, H_1 and H_9), 5.05 (m, 2H, H_3 and H_8), 7.10 (m, 1H, H_5 L), 7.31 (m, 1H, H_7 L), 7.41 (m, 1H, H_6 L), 7.65 (m, 1H, H_4 L), 10.12 and 10.64 (2H, NH and OH). $^{13}C\{^1H\}$ NMR (CD_2Cl_2): δ 21.1 (s, $2CH_3$), 36.7 (s, C_4 and C_5), 74.8 and 76.6 (s, C_1 and C_8), 95.5 and 97.2 (s, C_3 and C_6), 109.1 (s, C_7 L), 113.6 (s, C_{3a} L), 119.5 (s, C_5 L), 120.2 (s, C_4 L), 129.1 (s, C_6 L), 131.5 and 131.9 (s, C_2 and C_7), 142.8 (s, C_{7a} L), 163.0 (s, C_2 L).

Synthesis of Complex [Ru(η^3:η^3-$C_{10}H_{16}$)Cl(κ-*N*,*O*-2-(1*H*-pyrazol-3-yl)phenoxy)] (5). *Method a:* A solution of complex [Ru(η^3:η^3-$C_{10}H_{16}$)Cl_2(κ-*N*-2-(1*H*-pyrazol-3-yl)phenol)] (**2e**; 100 mg, 0.2 mmol) in dichloromethane was treated with an excess of NaOH. After 2 h, the solution was filtered off through Celite and the product purified by column chromatography (silica gel with dichloromethane as the eluent). Yield: 35% (32 mg). Anal. Calcd for $RuC_{19}H_{23}ClN_2O$: C, 52.83; H, 5.37; N, 6.49. Found; C, 52.65; H, 5.32; N, 6.45. IR (KBr, cm^{-1}): ν 594 (w), 659 (w), 765 (s), 849 (w), 1128 (m), 1315 (vs), 1440 (s), 1488 (s), 1521 (w), 1549 (w), 1595 (s), 2909 (w), 3137 (w), 3250 (vs). ^1H NMR (CD_2Cl_2): δ 2.02 and 2.37 (s, 6, $2CH_3$), 2.69 (m, 2H, H_4 and H_6), 3.26 (m, 2H, H_5 and H_7), 3.22 and 3.93 (s, 2H, H_2 and H_{10}), 4,25 and 4.48 (s, 2H, H_1 and H_9), 4.31 and 4.92 (m, 2H, H_3 and H_8), 6.52 (m, 1H, H_5 Ph), 6.56 (m, 1H, H_3 Ph), 6.82 (m, 1H, H_4 L), 6.92 (m, 1H, H_4 Ph), 7.45 (m, 1H, H_6 Ph), 7.80 (m, 1H, H_5 L), 12.13 (s, 1H, NH). $^{13}C\{^1H\}$ NMR (CD_2Cl_2): δ 18.3 and 20.5 (s, $2CH_3$), 36.3 and 36.9 (s, C_4 and C_5), 75.0 and 19.4 (s, C_1 and C_8), 98.6 and 103.5 (s, C_3 and C_6), 102.9 (s, C_4 L), 113.9 (s, C_5 Ph), 116.5 (s, C_2 Ph), 124.3 (s, C_3 Ph), 126.5 and 128.0 (s, C_2 and C_7), 127.7 (s, C_6 Ph), 129.5 (s, C_4 Ph), 131.3 (s, C_5 L), 131.4 (s, C_3 L), 149.6 (s, C_1 Ph). *Method b:* A solution of 2-(1*H*-pyrazol-3-yl)phenol (32 mg, 0.2 mmol) was treated with an excess of NaOH. After 1 h of agitation, complex **1** (61.6 mg, 0.1 mmol) was added to the solution. After 2 h, the solution was filtered off through Celite and the product purified by column chromatography (silica gel with dichloromethane as the eluent). Yield: 41% (38 mg).

X-ray Crystal Structure Determination of Complexes 2a−2c, 2e, 3, and 5. The most relevant crystal and refinement data are collected in Table 1.

In all cases, crystals suitable for X-ray diffraction analysis were obtained by the slow diffusion of hexane into a saturated solution of the complexes in dichloromethane.

Data collection was performed on an Oxford Diffraction Xcalibur Nova single-crystal diffractometer, using Cu Kα radiation (λ = 1.5418 Å; **2a**−**2c** and **5**). Images were collected at a 75 mm fixed crystal−detector distance, using the oscillation method, with 1° oscillation and variable exposure time per image (3−50 s). The data collection strategy was calculated with the program *CrysAlis Pro CCD*.[16] Data reduction and cell refinement were performed with the program *CrysAlis Pro RED*.[16] An empirical absorption correction was applied using the SCALE3 ABSPACK algorithm, as implemented in the program *CrysAlis Pro RED*.[16]

For **2e** and **3**, diffraction data were recorded on a Nonius Kappa CCD single-crystal diffractometer, using Mo Kα radiation (λ = 0.710 73 Å). Images were collected at a 35 mm fixed crystal−detector distance, using the oscillation method, with 1° oscillation and 50−100 s exposure time per image. The data collection strategy was calculated with the program *Collect*.[17] Data reduction and cell refinement were performed with the programs *HKL Denzo* and *Scalepack*.[18] A semiempirical absorption correction was applied using the program *SORTAV*.[19] The software package *WINGX*[20] was used for space group determination, structure solution, and refinement. The structures for complexes **2b**, **2c**, **2e**, and **3** were solved by Patterson interpretation and phase expansion using *DIRDIF*.[21] For **2a** and **5**, the structures were solved by direct methods using *SIR92*.[22] In the asymmetric unit of the crystal of **2a**, 1.5 molecules were found (**2aI** and 0.5**2aII**). In the molecule **2aII**, the atoms C19 and N4 are disordered in two positions with an occupancy factor of ca. 0.5. Isotropic least-squares refinement on F^2 using *SHELXL97*[23] was performed.

During the final stages of refinement, all of the positional parameters and anisotropic temperature factors of all of the non-H atoms were refined. For **2a**, **2e**, and **3**, the H atoms were geometrically located and their coordinates were refined by riding on their parent atoms. For **2b**, **2e**, and **5** (as well as H4N, H19, H1a, H1b, H10a, and H10b for **2a** and H1a, H1b, H10a, and H10b for **2e** and **3**), the coordinates of the H atoms were found from different Fourier maps and included in a refinement with isotropic parameters.

The function minimized was $([\Sigma w(F_o^2 - F_c^2)/\Sigma w(F_o^2)]^{1/2}$, where $w = 1/[\sigma^2(F_o^2) + (aP)^2 + bP]$ (a and b values are collected in Table 1)

Table 1. Crystallographic Data for Compounds of 2a−2c, 2e, 3, and 5

	2a	2b	2c	2e	3	5
chemical formula	$C_{13}H_{20}Cl_2N_2Ru$	$C_{14}H_{22}Cl_2N_2Ru$	$C_{15}H_{24}Cl_2N_2Ru$	$C_{19}H_{24}Cl_2N_2ORu$	$C_{13}H_{19}Cl_2N_3O_2Ru$	$C_{19}H_{23}ClN_2ORu$
fw	376.28	390.31	404.33	486.37	421.28	431.91
T, K	293(2)	293(2)	293(2)	293(2)	293(2)	293(2)
wavelength, Å	1.5418	1.5418	1.5418	0.7107	1.5418	1.5418
space group	*Fdd*2	$Pna2_1$	$P2_1/c$	$P2_1/c$	$P2_1/c$	*Pbca*
a, Å	33.2559(8)	7.6952(1)	9.1513(1)	16.2255(8)	12.3933(7)	8.8541(1)
b, Å	24.4116(6)	22.8324(3)	22.9768(2)	8.3163(4)	8.5805(4)	13.8896(1)
c, Å	11.1014(2)	9.0117(1)	7.8822(1)	14.5735(4)	15.8735(10)	29.3729(2)
α, deg	90	90	90	90	90	90
β, deg	90	90	93.313(1)	91.335(3)	95.632(3)	90
γ, deg	90	90	90	90	90	90
Z	24	4	4	4	4	8
V, Å^3	9012.4(3)	1583.35(3)	1654.60(3)	1965.96(15)	1679.85(16)	3612.28(5)
ρ_{calcd}, g cm^{-3}	1.664	1.637	1.623	1.582	1.666	1.588
μ, mm^{-1}	11.586	11.014	10.562	1.079	1.258	8.441
GOF on F^2	1.019	1.083	1.067	0.866	0.956	1.035
weight function (a, b)	0.0195, 8.5210	0.0689, 0.0	0.0691, 0.0677	0.0474, 0.0	0.0541, 0.0	0.0355, 1.3321
R1[a] [$I > 2\sigma(I)$]	0.0426	0.0329	0.0347	0.0375	0.0336	0.0235
wR2[a] [$I > 2\sigma(I)$]	0.1151	0.0904	0.0920	0.1009	0.0922	0.0613
R1[a] (all data)	0.0443	0.0343	0.0386	0.0645	0.0494	0.0255
wR2[a] (all data)	0.1169	0.0915	0.0949	0.1068	0.1119	0.0629
F(000)	4560	792	824	952	848	1760

[a] $R1 = \Sigma(|F_o| - |F_c|)/\Sigma|F_o|$; $wR2 = \{\Sigma[w(F_o^2 - F_c^2)^2]/\Sigma[w(F_o^2)^2]\}^{1/2}$.

with $\sigma^2(F_o^2)$ from counting statistics and $P = [\max(F_o^2, 0) + 2F_c^2]/3$. Atomic scattering factors were taken from the International Tables for X-ray Crystallography.[24] Geometrical calculations were made with *PARST*.[25] The crystallographic plots were made with *PLATON*[26] and *ORTEP-3 for Windows*.[27]

Theoretical Calculations. The theoretical calculations were performed using the program package *Gaussian03*[28] at the density functional theory (DFT) level by means of the hybrid B3LYP functional.[29] In all geometry optimizations, Pople's 6-31G(d) split-valence basis set was used for N, C, H, O, and Cl elements and LANL2DZ,[30] for Ru which combines quasi-relativistic effective core potentials with a valence double-basis set. Frequency calculations were performed to determine whether the optimized geometries were minima on the potential energy surface. The energy in the solvent was estimated by the application of single-point calculations using the polarizable continuum model (PCM) with standard UA0 solvation spheres and the extended basis set 6-311++G(d,p) on the optimized stationary points in CH_2Cl_2 ($\varepsilon = 8.93$).[31]

NMR Studies. The NMR spectra were recorded on a Bruker AV 600 spectrometer operating at 600.15 and 150.91 MHz for ^{1}H and ^{13}C, respectively, using a 5 mm PATXI-^{1}H/D-^{13}C/^{15}N inverse probe with a z-gradient coil or on a Bruker AV 400 spectrometer operating at 400.13 and 100.61 MHz for ^{1}H and ^{13}C, respectively, using a 5 mm TBO-^{1}H/X-BB/^{31}P/D direct probe with a z-gradient coil. All of the experiments were acquired and processed with *TOPSPIN 1.3* Bruker NMR software. The two-dimensional NMR experiments were recorded on the AV 600 spectrometer using gradient-enhanced versions of the pulse sequences. The ^{1}H DOSY experiments were performed on the AV400 spectrometer. The gradient unit of the spectrometer produced magnetic-field pulsed gradients in the z axis of 53.5 G cm^{-1}. The gradient strength was calibrated using a D_2O sample to obtain a diffusion coefficient of 1.90×10^{-9} m^2 s^{-1} for HDO. During the DOSY experiments, the temperature was set to 298 K and maintained with an air flow of 400 L h^{-1}. The experiments were acquired with the bipolar longitudinal eddy current delay pulse program (*ledbpgps2s* in Bruker software) with spinning of the sample to avoid convection influence.[32] The diffusion time (D20) and gradient duration (P30) were previously optimized with the *ledbpgp2s1d* sequence for each measurement to get 1−5% of the residual signal with maximum strength while observing a progressive decay of the signal intensities. For a typical ^{1}H DOSY experiment, P30 = 0.9−1.0 ms and D20 = 120 ms, an eddy current delay (T_e) of 5 ms, and a spoil gradient (P19) of 0.8 ms were used. The pulse gradients were increased from 2 to 95% of the maximum strength in a linear ramp through 16 steps of 16K data points each. The size of the flame ionization detector was 16K, the spectral width was set to AQ = 1.5 s, the number of scans were 16−32, and a relaxation delay D1 = 1 s was used; the direct dimension was zero-filled to 32K, Fourier-transformed, and phase-corrected. The diffusion dimension was zero-filled to 128 and processed with the standard Bruker DOSY algorithm. The diffusion coefficients were measured in a logarithmic scale, and the accuracy of the reported values is ±0.01. **NMR Data at 183 K for Complex 3.** ^{1}H NMR (600.15 MHz, CD_2Cl_2, 183 K): δ 11.75 (bs, 1H, NH-2), 11.23 (bs, 1H, NH-4), 8.62 (s, 1H, CH), 5.30 (m, 1H, internal allylic), 5.24 (m, 1H, internal allylic), 4.89 (s, 1H, terminal allylic), 4.73 (s, 1H, terminal allylic), 4.33 (s, 1H, terminal allylic), 4.22 (s, 1H, terminal allylic), 3.06 (m, 2H, aliphatic CH_2), 2.36 (m, 2H, aliphatic CH_2), 2.30 (s, 6H, CH_3). ^{13}C{^{1}H} NMR (150.91 MHz, acetone-d_6, 183 K): δ 155.3 (C, C-5), 148.2 (C, C-3), 143.7 (CH, C-6), 133.3 (C, allylic), 96.3 (CH, allylic), 94.6 (CH, allylic), 77.1 (CH_2, allylic), 36.6 (CH_2, aliphatic), 36.4 (CH_2, aliphatic), 21.9 (CH_3), 21.8 (CH_3). **NMR Data in the Presence of DMSO-d_6 at 298 K.** ^{1}H NMR (600.15 MHz, CD_2Cl_2, 298 K): δ 11.70 (bs, 1H, NH-2), 11.26 (bs, 1H, NH-4), 7.27 (d, J_{HH} = 1.6 Hz, 1H, CH-6), 5.13 (m, 2H, internal allylic), 4.72 (s, 2H, terminal allylic), 3.99 (s, 2H, terminal allylic), 3.20 (m, 2H, aliphatic CH_2), 2.57 (m, 2H, aliphatic CH_2), 2.32 (s, 6H, CH_3). ^{13}C{^{1}H} NMR (150.91 MHz, acetone-d_6, 298 K): δ 157.3 (C, C-5), 149.1 (C, C-3), 135.4 (CH, C-6), 129.6 (C, allylic), 102.3 (CH, allylic), 75.3 (CH_2, allylic), 35.5 (CH_2, aliphatic), 20.5 (CH_3).

dx.doi.org/10.1021/ic200547k |*Inorg. Chem.* 2011, 50, 4868–4881

Scheme 1

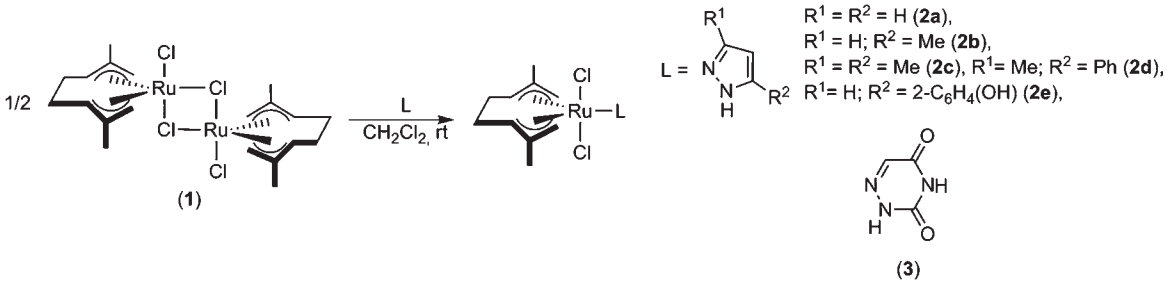

RESULTS AND DISCUSSION

With the aim of providing ruthenium(IV) complexes featuring hydrogen bonding via N−H groups, we have selected the pyrazole derivatives 6-azauracil and 1,2-dihydro-indazol-3-one as typical heterocycles acting as two-electron N-donor ligands. The presence of additional functionalities such as OH and C═O groups can supply complementary effects. The use of dimer **1** as the starting material for the direct synthesis of the target complexes stems from the following: (i) it is a readily and/or commercially available material;[33] (ii) it is an excellent precursor of the unsaturated 16-electron fragment *trans*-[Ru(η^3:η^3-$C_{10}H_{16}$)-Cl_2], which enables the binding of two-electron N ligands;[34] (iii) the resulting complexes provide a *trans*-$RuCl_2$ disposition, which is prone to generating favorable intra- and intermolecular Cl···H hydrogen bonding.

Synthesis of [Ru(η^3:η^3-$C_{10}H_{16}$)Cl_2L] [L = Pyrazole (2a),[15] 3-Methylpyrazole (2b), 3,5-Dimethylpyrazole (2c), 3-Methyl-5-phenylpyrazole (2d), 2-(1*H*-Pyrazol-5-yl)phenol (2e), and 6-Azauracil (3)]. The treatment of **1** with 2 equiv of the appropriate pyrazole derivative, 2-(1*H*-pyrazol-3-yl)phenol or 6-azauracil, in dichloromethane or dichloromethane/methanol at room temperature affords the corresponding mononuclear complexes **2a**−**2e** and **3**. All complexes have been isolated (43−86%) as air-stable orange solids (Scheme 1).

Compounds **2a**−**2e** and **3** are soluble in dichloromethane and acetone and insoluble in hexane and diethyl ether. In contrast to **2a**−**2e**, complex **3** is soluble in water. Although conductivity measurements of acetone solutions show that there are no electrolytes, the molar conductivity found for **3** in water is 177 Ω^{-1} cm^2 mol^{-1}, a value that is among those expected for 1:1 or 2:1 electrolytes (118−131 and 235−273 Ω^{-1} cm^2 mol^{-1}, respectively). This seems to indicate that water−chloride exchange processes leading to an equilibrium containing cationic aqua species of the type [Ru(η^3:η^3-$C_{10}H_{16}$)Cl(6-azauracile)(H_2O)]$^+$ and [Ru(η^3:η^3-$C_{10}H_{16}$)(6-azauracile)$(H_2O)_2$]$^{2+}$ may be formed. Unfortunately, all attempts to isolate these species have been unsuccessful. Interestingly, the aqueous solution is acidic with a pH value of 4.0, indicating that proton dissociation either from the coordinated water molecule or the uracile N−H group can also take place. Spectroscopic data (IR and NMR spectroscopy) and elemental analysis are in agreement with the proposed formulations. In particular, ^{1}H and ^{13}C{^{1}H} NMR spectra (CD_2Cl_2) of complexes **2a**−**2e** and **3** show the signals for the η^3:η^3-2,7-dimethylocta-2,6-diene-1,8-diyl ligand, which compare well with those previously reported for analogous complexes containing monodentate nitrogen ligands.[34] It is worth noting that proton and carbon resonances of the 2,7-dimethylocta-2,6-diene-1,8-diyl group in the NMR spectra are in accordance with the formation of a simple equatorial adduct with C_2 symmetry in which the halves of the bis(allyl) ligand are in equivalent environments.[34] In addition, the spectra display the expected signals for the nitrogen ligands (see the Experimental Section for details). Significantly, IR and ^{1}H NMR spectra are consistent with the κ-N coordination of pyrazole ligands and 6-azauracil, i.e., ν(N−H) absorption band (KBr) at 3222−3312 (**2b**−**2e**) and 3430 (**3**) cm^{-1}; δ N−H resonance at 11.21−12.85 (**2b**−**2e**) and 11.74 and 9.10 (**3**). Further NMR data of complex **3** prove the existence of dimeric association in solution through intermolecular hydrogen bonding (see below).

Scheme 2

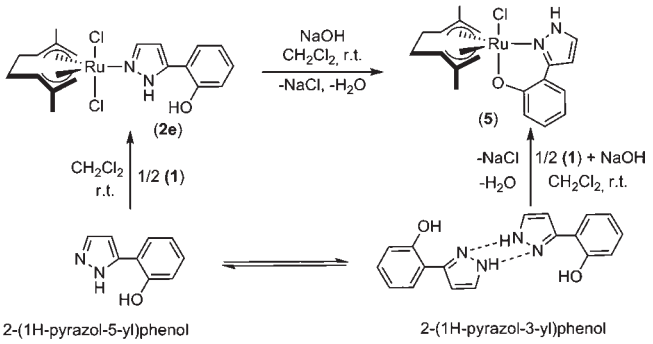

It is interesting to note that the formation of complex **2e** proceeds through tautomerization of the ligand-free 2-(1*H*-pyrazol-3-yl)phenol into the coordinated 2-(1*H*-pyrazol-5-yl)-phenol (Scheme 2). This is consistent with the well-known tautomerism of diazoles via intermolecular proton transfer,[35] although intramolecular tautomerization via the ruthenium complex bearing a 2-(1*H*-pyrazol-3-yl)phenol ligand cannot be ruled out. The structure of **2e** in the solid state determined by X-ray diffraction (see below) confirms the presence of the 2-(1*H*-pyrazol-5-yl)phenol ligand.

Synthesis of [Ru(η^3:η^3-$C_{10}H_{16}$)Cl_2(1*H*-indazol-3-ol)] (4). By following an analogous synthetic procedure, complex **4** was obtained by the reaction of **1** with 1,2-dihydroindazol-3-one (Scheme 3). It has been isolated as an air-stable orange solid (47%), which is soluble in chlorinated solvents and acetone and insoluble in water, hexane, and diethyl ether.

Complex **4** has been characterized by elemental analysis and spectroscopic methods (IR and ^{1}H and ^{13}C{^{1}H} NMR). In particular, proton and carbon spectra reveal that the halves of the 2,7-dimethylocta-2,6-diene-1,8-diyl ligand are now in an inequivalent environment (i.e., a six-line pattern of 74.8, 76.6, 95.5, 97.2,

dx.doi.org/10.1021/ic200547k |*Inorg. Chem.* 2011, 50, 4868–4881

Scheme 3

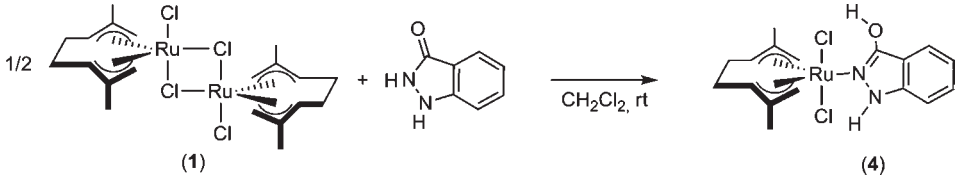

Scheme 4

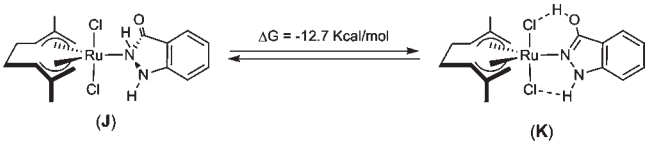

131.5, and 131.9 ppm is observed for the skeletal allyl groups in the ^{13}C NMR spectrum). In addition, the IR spectrum (KBr) shows the disappearance of the typical ν(C═O) absorption of the free ligand at 1620 cm^{-1}, also displaying new ν(C═N) and ν(O−H) absorptions at 1624 (w) and 3446 (vs and br) cm^{-1}, respectively. These data are consistent with the presence of the iminic tautomer form of 1,2-dihydroindazol-3-one, namely, 1*H*-indazol-3-ol (**K**, Scheme 4). This is probably promoted by the coordination to ruthenium via the formation of intramolecular Cl···H−O and Cl···H−N bonds.

Theoretical calculations of the stabilization energy of tautomeric forms of complex **4** have been analyzed by B3LYP DFT studies. Optimized geometries of the complexes are depicted in the Supporting Information. They have been obtained by using bond lengths and angles from the X-ray data of analogous complexes herein described (see below). Frequency calculations for the optimized geometries have been performed and are consistent with minima on the potential energy surface. It is found that the proposed coordination of tautomer **K** stabilizes the resulting complex **4** in 12.7 kcal mol^{-1} with respect to that of 1,2-dihydroindazol-3-one (**J**).

All attempts to obtain suitable crystals of **4** for X-ray diffraction studies have been unsuccessful. Nevertheless, the optimized geometries display the expected N−H/O-H···Cl hydrogen bonding (see the Supporting Information).

Synthesis of [Ru(η^3:η^3-$C_{10}H_{16}$)Cl(κ^2-*N*,*O*-2-(1*H*-pyrazol-3-yl)phenoxy)] (5). The preparation of complex **2e** containing the N-coordinated ligand 2-(pyrazol-5-yl)phenol raises the question of whether the expected deprotonation reaction of the hydroxyl group could lead to a chelate complex (Scheme 2). Thus, the treatment of **1** with an equivalent amount of 2-(1*H*-pyrazol-3-yl)phenol in the presence of NaOH in dichloromethane leads to the formation of complex **5**, which is isolated after chromatographic purification as an air-stable orange solid (41%). Alternatively, the treatment of **2e** with an excess of NaOH in dichloromethane also leads to the formation of complex **5** (35%; Scheme 2).

Compound **5** is soluble in chlorinated solvents and acetone and insoluble in water, hexane, and diethyl ether. Elemental analysis and spectroscopic methods (IR and ^1H and $^{13}C\{^1H\}$ NMR) of complex **5** are in accordance with the proposed formulation and with the formation of the chelate ring. This is evidenced in the IR (KBr) spectrum by the disappearance of the ν(OH) absorption and in the $^{13}C\{^1H\}$ NMR spectrum, which shows 10 different signals of the 2,7-dimethylocta-2,6-diene-1,8-diyl ligand, as is expected for the loss of C_2 symmetry. The X-ray crystal structure of complex **5** (see below) confirms the formation of the metalla-2-(1*H*-pyrazol-3-yl)phenoxy chelate ring.

X-ray Crystal Structures. The structures of complexes **2a**−**2c**, **2e**, **3**, and **5** have been determined by X-ray crystallography in the solid state. Collection data are summarized in Table 1, and selected bond distances and angles are shown in Table 2. For complex **2a**, two independent molecules were found in the unit cell, so in this case, two sets of values are shown. Drawings of the molecular structures are depicted in Figures 2−7. Figures 8−12 provide views of the closest intermolecular hydrogen bonds for complexes **2a**−**2c**, **2e**, and **3**.

As a general trend, the geometry about the ruthenium(IV) center can be described as a distorted trigonal bipyramid by considering the allyl groups as monodentate ligands bound to ruthenium through their centroids C*1 and C*2, showing the expected η^3:η^3-coordination mode. The structures of complexes **2a**−**2c**, **2e**, and **3** (Figures 2−6) feature the two chloride ligands axially located in a formal trans disposition with slight deviations of the Cl1−Ru−Cl2 angle from ideal 180° [in the range of 170.31(8)−172.45(5)°]. Cl1−Ru−N1 and Cl2−Ru−N1 bonding angles along with bond distance values C−C and Ru−C [in the range of Ru−C*1 = 1.9959(4)−2.0145(2) Å and Ru−C*2 = 1.9960(4)−2.0126(2) Å] compare well with those observed in other structures containing the "Ru(η^3:η^3-$C_{10}H_{16}$)" unit.[36] All of the ligands are coordinated edge-on via the iminic N atom, which resides in an equatorial position along with the allyl groups. The Ru−N bond length values are in the range of 2.142(6)−2.193(3) Å, which can be compared with those reported in the literature.[36] A significant feature is concerned with the observed dihedral angle α formed by the corresponding planes containing the Ru−N−N−H skeleton of the heterocyclic rings and the Cl−Ru−Cl moiety. This angle arises from the folded position of the plane containing either the pyrazole (**2a**−**2c** and **2e**) or 6-azauracil (**3**) rings. With the exception of the angle found in one of the independent molecules of **2a** [e.g., 1.4(12)°], the rest of the values are in the range of 11.5−36.7(2)°. The folding of the heterocyclic rings with respect to the molecular plane appears to locate the N−H vector in such a way that the *intramolecular* hydrogen bonding is maximized (see below).

The structure of complex **5** is shown in Figure 7 (selected bonding parameters appear in the caption). The structure can also be described as a distorted trigonal-bipyramidal geometry in which the centroids C*1 and C*2 and N1 occupy the equatorial sites and Cl1 and O1 the axial sites. Structural relevant parameters are related to the presence of the chelate six-membered ring, which displays internal angles and bond distances with no appreciable changes compared to its precursor **2e**. The Ru−O1 [2.0852(13) Å] and Ru−Cl1 [2.4139(5) Å] bond lengths compare

dx.doi.org/10.1021/ic200547k |*Inorg. Chem.* 2011, 50, 4868–4881

Table 2. Main Bond Lengths (Å), Angles (deg), and Dihedral Angle α (deg) between the Ru−Cl and N−N Bonds in Complexes 2a−2c, 2e, and 3

	Ru−C*1[a]	Ru−C*2[a]	Ru−Cl1	Ru−Cl2	Ru−N1	Cl1−Ru−Cl2	Cl1−Ru−N1	Cl2−Ru−N1	Cl1−Ru−N1−N2 (α)[b]
2a[c]	2.004(9), 2.001(9)	2.005(9)	2.4092(17), 2.4193(17)	2.4193(1)	2.172(7), 2.181(9)	170.31(8), 170.96(11)	85.19(17), 85.48(5)	85.12(17)	21.3(6), 1.4(12)
2b	2.00(2)	2.011(6)	2.4323(11)	2.4060(10)	2.142(6)	171.11(6)	85.19(12)	85.94(12)	39.9(5)
2c	2.0145(2)	2.0126(2)	2.4337(6)	2.4109(7)	2.193(3)	173.15(3)	84.89(6)	88.54(6)	36.7(2)
2e	2.0113(4)	2.0098(4)	2.4196(15)	2.4243(14)	2.159(5)	171.57(6)	85.21(13)	86.42(13)	24.3(3)
3	1.9959(4)	1.9960(4)	2.3986(14)	2.4066(14)	2.231(4)	172.45(5)	85.48(12)	86.98(12)	11.5(3)

[a] C*1 = centroid of the allylic groups C1, C2, and C4; C*2 = centroid of the allylic groups C7, C8, and C10. [b] Dihedral angle α between the "RuClN" and ligand planes. [c] Two independent molecules in the unit cell.

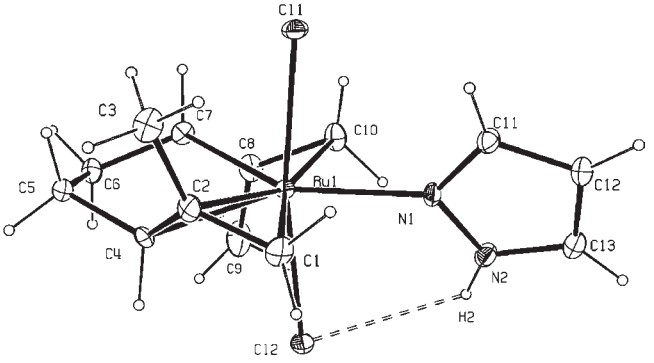

Figure 2. ORTEP-type view of the structure of complex **2aI**, showing the crystallographic labeling scheme and N−H···Cl intramolecular hydrogen bond. Thermal ellipsoids are drawn at the 10% probability level.

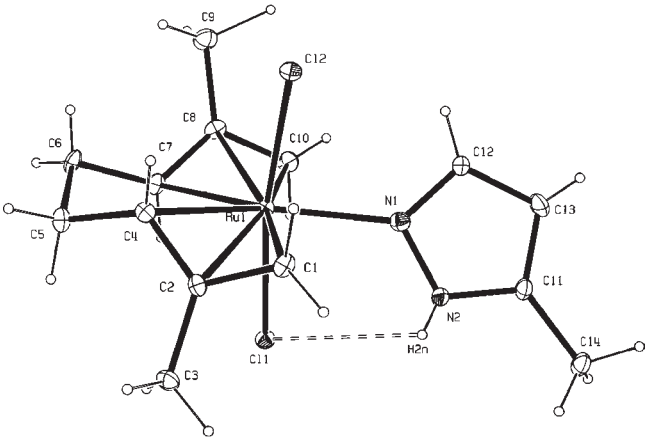

Figure 3. ORTEP-type view of the structure of complex **2b**, showing the crystallographic labeling scheme and the N−H···Cl intramolecular hydrogen bond. Thermal ellipsoids are drawn at the 10% probability level.

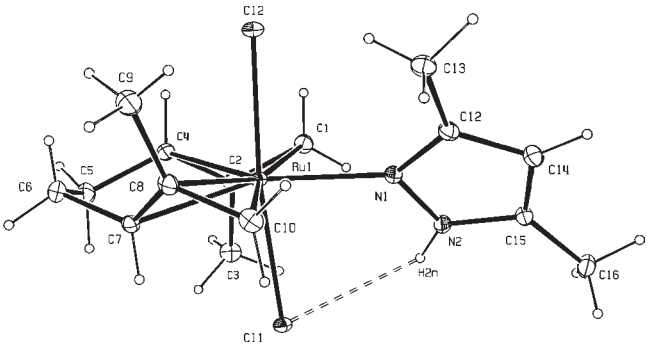

Figure 4. ORTEP-type view of the structure of complex **2c**, showing the crystallographic labeling scheme and the N−H···Cl intramolecular hydrogen bond. Thermal ellipsoids are drawn at the 10% probability level.

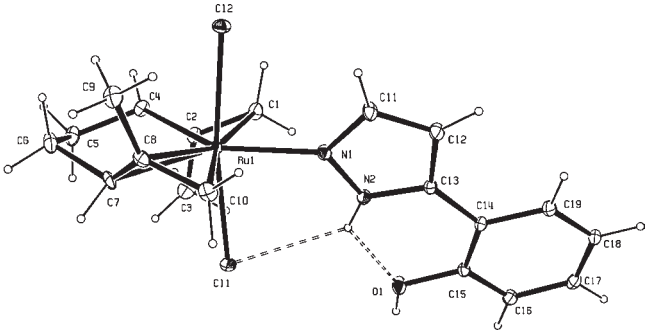

Figure 5. ORTEP-type view of the structure of complex **2e**, showing the crystallographic labeling scheme and N−H···Cl and N−H···O intramolecular hydrogen bonds. Thermal ellipsoids are drawn at the 10% probability level. Selected bond distances (Å) and angles (deg): N1−C13 = 1.271(7), C13−C14 = 1.500(8), C14−C19 = 1.416(3), C19−O1 = 1.318(6); Ru−N1−C13 = 116.8(3), N1−C13−C14 = 117.0(5), C13−C14−C19 = 129.7(5), C14−C19−O1 = 117.9(5).

well to those shown by the other ruthenium(IV) complexes herein described and other complexes containing Ru−O alkoxides.[37] The remaining structural parameters related to the expected η^3:η^3-coordination mode of the diallyl group $C_{10}H_{16}$ are similar to those of the complexes described above.

Hydrogen Bonding. All molecular structures examined show that the ligand N−H hydrogen (located on an equatorial site) is involved in a hydrogen bond with one of the chloride ligands in the axial position.[15a,38] Distances between the N−H hydrogen and the chloride are in the range 2.27(5)−2.78 Å and angles N2−H−Cl1 lie in the range 102−138° (see Table 3). Despite the fact that angles are rather small compared to those in optimal hydrogen bonding (closer to 180°),[39] these values along with the observed dihedral angle α (Table 2) are consistent with the existence of *intramolecular* hydrogen bonds.

The unit cell packing diagrams of complexes **2a**−**2c**, **2e**, and **3** shown in Figures 8−12 are particularly illustrative of the ability of

dx.doi.org/10.1021/ic200547k |*Inorg. Chem.* 2011, 50, 4868–4881

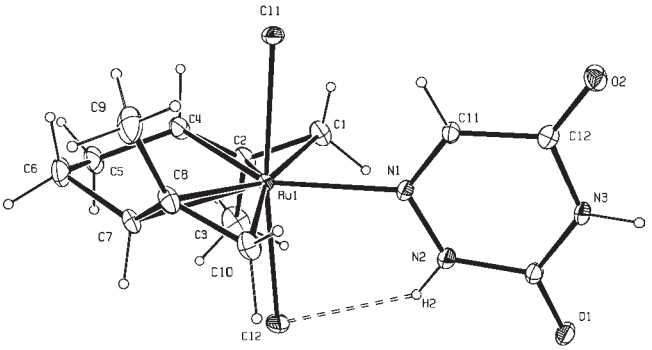

Figure 6. ORTEP-type view of the structure of complex **3**, showing the crystallographic labeling scheme and the N−H···Cl intramolecular hydrogen bond. Thermal ellipsoids are drawn at the 10% probability level.

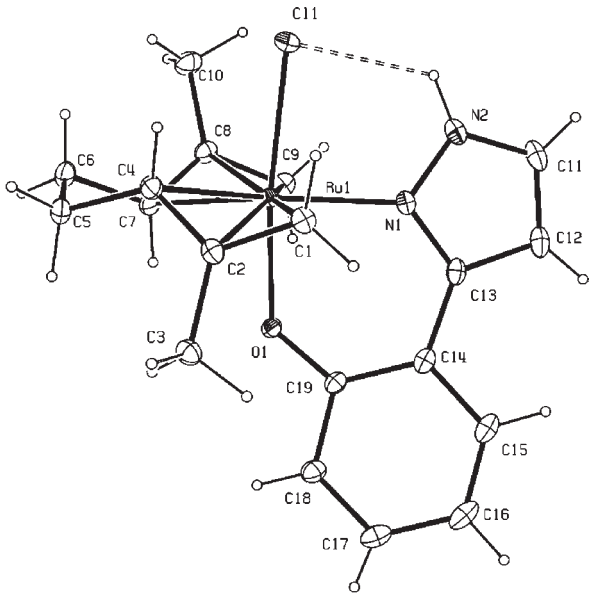

Figure 7. ORTEP-type view of the structure of complex **5**, showing the crystallographic labeling scheme and the N−H···Cl intramolecular hydrogen bond. Thermal ellipsoids are drawn at the 10% probability level. Selected bond distances (Å) and angles (deg): Ru1−C*1 = 1.99519(14), Ru1−C*2 = 1.99289(14), Ru1−Cl1 = 2.4139(5), Ru1−O1 = 2.0852(13), Ru1−N1 = 2.0982(16), N2−H(N2) = 0.94(4); C*1−Ru1−C*2 = 132.761(7), C*1−Ru1−N1 = 114.26(5), C*2−Ru1−N1 = 112.87(5), C*1−Ru1−O1 = 94.54(4), C*2−Ru1−O1 = 85.65(4), N1−Ru1−O1 = 86.03(6), C*1−Ru1−Cl1 = 95.381(16), C*2−Ru1−Cl1 = 90.114(16), N1−Ru1−Cl1 = 86.86(5), O1−Ru1−Cl1 = 172.64(4); N1−C13 = 1.332(3), C13−C14 = 1.458(3), C14−C19 = 1.519(8), C19−O1 = 1.322(2); Ru−N1−C13 = 123.31(15), N1−C13−C14 = 122.64(12), C13−C14−C19 = 123.25(19), C14−C19−O1 = 125.55(19), C19−O1−Ru = 124.82(12), O1−Ru−N1 = 83.03(06) (C*1 = centroid of the allylic groups C1, C2, and C4; C*2 = centroid of the allylic groups C7, C8, and C10).

these complexes to participate also in intermolecular contacts. The distances between coordinated heterocyclic N−H and the neighboring chloride ligands are somewhat similar to the intramolecular ones [2.00−2.77 Å vs 2.27(5)−2.78 Å; Table 3]. In contrast, values of the angles N−H···Cl are greater (132−198.7° vs 102−138°), supporting the existence of intermolecular contacts. These interactions may play a significant role in the bifunctional activation of substrates.

The packing diagram of the uracil complex **3** (Figure 12) is exceptional because it shows a pairing of molecular units via two intermolecular N−H···O=C interactions. The distance and angle of the N−H···O contact of 2.00 Å and 162°, respectively, allow it to be classified as "moderate" among those considered most common in chemical systems.[39]

NMR Diffusion Studies. In order to investigate the existence in solution of the intra- and intermolecular hydrogen bonds detected in the analysis of the X-ray structures, we have carried out a thorough NMR study for complex **3** as a model, including structure elucidation, variable-temperature measurements, and DOSY experiments.

The integrals of the room temperature ^{1}H NMR spectrum (CD_2Cl_2) of complex **3** account for 1:1 octadienediyl/6-azauracil fragments, showing single resonances for all chemically equivalent protons, as is also observed in the ^{13}C NMR spectrum (CD_2Cl_2). This feature indicates that the 6-azauracil ligand has been incorporated into the equatorial position of the ruthenium center and a free rotation about the Ru−N bond, thus achieving equivalent environments for the halves of the 2,7-dimethyloctadienediyl group. The proton signals for 6-azauracil appear as three broad singlets at 11.74, 9.10, and 8.65 ppm. The HSQC spectrum identifies the iminic proton at 8.65 ppm and sets two more deshielded signals for the NH protons. Because their high chemical shifts may be indicative of the participation of these NH protons in some type of hydrogen bonding, we have carried out several studies by varying the temperature, solvent, and concentration in order to elucidate the bonding nature of these exchangeable protons.

First, we prepared several NMR samples with different concentrations (5, 12, 18, and 24 mM in CD_2Cl_2). Their ^{1}H NMR spectrum showed that the signal at 11.74 ppm remains unaffected in all cases, while the signal at 9.10 ppm is shifted to lower fields with increasing concentration. This concentration dependence clearly points out to intermolecular hydrogen bonding for the signal at 9.10 ppm and an intramolecular nature for the proton at 11.74 ppm. This assumption is also supported by the NOESY spectrum of complex **3**, which shows an exchange cross peak with residual water for the NH proton at 9.10 ppm, which is not detectable for the signal at 11.74 ppm. The unambiguous assignment of the signal at 9.10 ppm for the NH-4 proton and the signal at 11.74 ppm for the NH-2 through 2D NMR experiments at low temperature confirms the existence of an intramolecular hydrogen bond between NH-2 and a Cl atom of the coordination sphere of the metal.[40]

In a next step, we have studied the influence of the temperature. The ^{1}H NMR spectrum of complex **3** (CD_2Cl_2) was recorded for a range of temperatures from 298 to 183 K. The analysis of the spectra showed that the signal for NH-4 (9.10 ppm) shifts to lower fields with decreasing temperature, while the chemical shift for the NH-2 proton (11.74 ppm) remains unaffected (Figure 13). This behavior of the NH resonances is in agreement with their respective exchangeable and nonexchangeable character already detected in the variable concentration study. Besides, there are other noticeable changes taking place when the temperature is decreased: the allylic signals of the 2,7-dimethyloctadienediyl group slowly broaden at 213 K and they split into two sets of signals; on the other hand, the broad signals for the iminic and NH-2 protons at 8.65 and 11.74 ppm become sharp singlets. The compound was characterized at 183 K. At that temperature, the ^{13}C NMR spectrum also shows splitting for some signals of the octadienediyl fragment: the aliphatic CH_2,

dx.doi.org/10.1021/ic200547k |*Inorg. Chem.* 2011, 50, 4868–4881

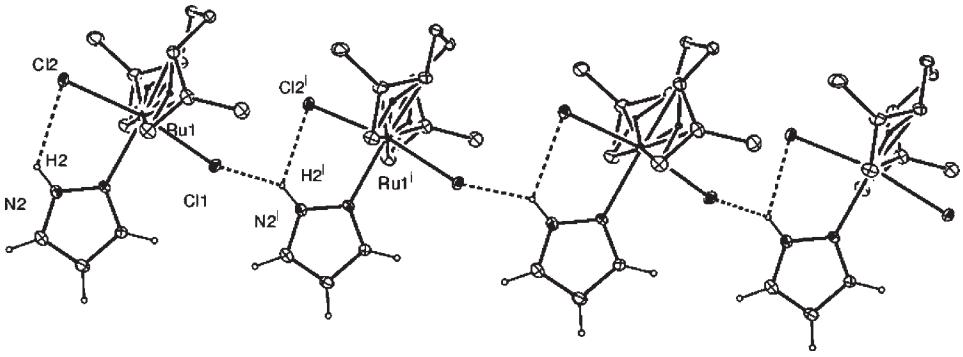

Figure 8. Inter- and intramolecular hydrogen bonds observed in the packing structure of complex **2aI**. All H atoms are excluded except those of the pyrazole ring.

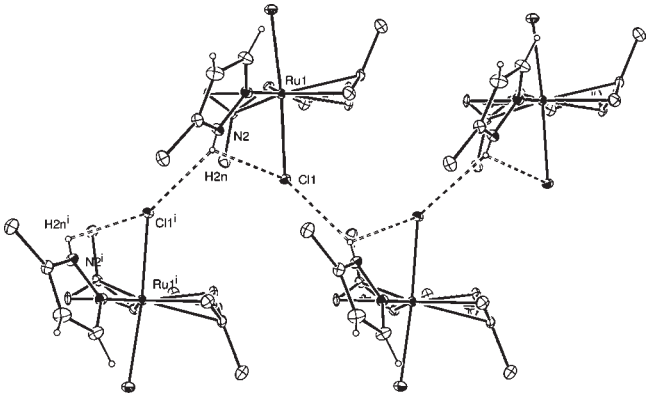

Figure 9. Inter- and intramolecular hydrogen bonds observed in the packing structure of complex **2b**. All H atoms are excluded except those of the pyrazole ring.

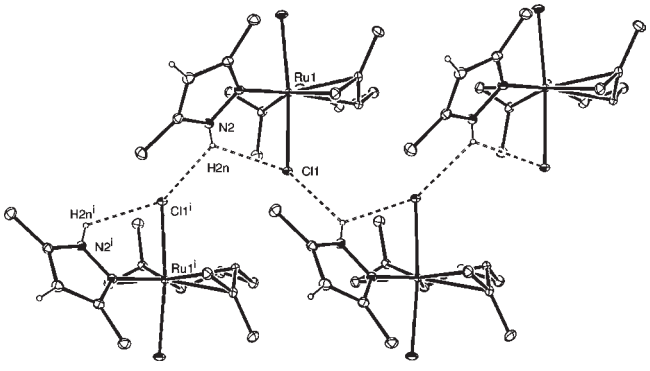

Figure 10. Inter- and intramolecular hydrogen bonds observed in the packing structure of complex **2c**. All H atoms are excluded except those of the pyrazole ring.

the internal allylic CH, and the methyl groups. This new situation indicates that at 183 K complex **3** is in the slow exchange zone, with restricted rotation around the Ru−N bond forced by the intramolecular hydrogen bond. Complete assignment of the ^{1}H and ^{13}C NMR spectra was achieved after inspection of the HSQC, HMBC, and the ROESY spectra at 183 K: the ROESY and HMBC cross peaks of the NH-2 and iminic protons led to the unambiguous assignment of the two amino protons.

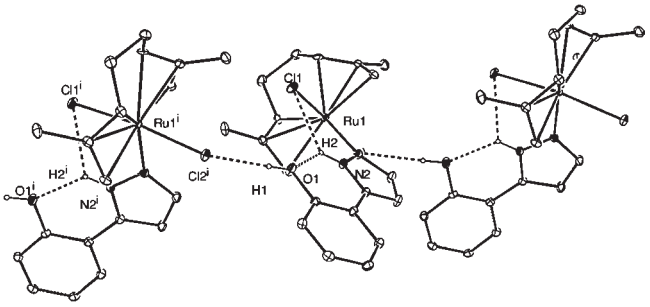

Figure 11. Inter- and intramolecular hydrogen bonds observed in the packing structure of complex **2e**. All H atoms are excluded except those of the N−H and O−H groups.

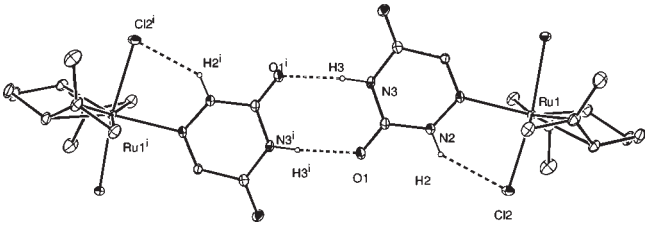

Figure 12. Inter- and intramolecular hydrogen bonds observed in the packing structure of complex **3**. All H atoms are excluded except those of the N−H groups.

The above-discussed NMR experiments prove the existence of an intramolecular hydrogen bond upon solution of complex **3** in a poorly coordinating solvent such as CH_2Cl_2. However, because the intermolecular hydrogen bonds could just as well involve dimeric structures arising from hydrogen bonds between the uracil groups of two molecules, we carried out several DOSY experiments to evaluate the size of the molecules present in solution.

DOSY[41] is an extremely useful NMR technique capable of estimating the size of a molecule in solution from its diffusion coefficient. It has been successfully applied in the identification and study of hydrogen-bond interactions[42] and chemical exchange.[43] The measured diffusion coefficient of the molecule in the NMR sample is a translational property, which the Stokes−Einstein equation[44] relates to the hydrodynamic radius of the molecule in solution. If the measurement is carried out in the presence of a reference compound, then an inverse relationship between the

dx.doi.org/10.1021/ic200547k |*Inorg. Chem.* 2011, 50, 4868–4881

Table 3. Hydrogen-Bonding[a] Contacts[b] in Complexes 2a−2c, 2e, 3, and 5 (Å and deg)

	intramolecular			intermolecular		
	D−H···A	H···A distance	D−H···A angle	D−H···A	H···A distance	D−H···A angle
2aI	N2−H···Cl2	2.56	118	N2−H···Cl1^{i}	2.59	132
2aII	N4−H···Cl3	2.67	102			
2b	N2−H···Cl1	2.78	114	N2−H···Cl1^{i}	2.71	152
2c	N2−H···Cl1	2.55(4)	123(3)	N2−H···Cl1^{i}	2.77(4)	198.7(12)
2e	N2−H···Cl1	2.43(5)	122(5)	O1−H···Cl2^{i}	2.45(5)	174(5)
	N2−H···O1	2.27(5)	138(5)			
3	N2−H···Cl2	2.30	137	N3−H···O1^{i}	2.00	162
5	N2−H···Cl1	2.42	124			

[a] A hydrogen bond exists between D−H and an atom A if (1) it constitutes a local bond and (2) X−H acts as proton donor to A.[39] [b] Weak hydrogen bonding of the type C−H···Cl is also detected but is not included in the table.

ratio of the diffusion coefficients and the hydrodynamic radii ($D_a/D_b = r_{Hb}/r_{Ha}$) can be established. Considering that the two molecules have a spherical shape, this relationship can be extended to a molecular weight ratio[45] between the two molecules: $(D_a/D_b = MW_b/MW_a)^{1/3}$.

The known complex $[Ru(\eta^3{:}\eta^3\text{-}C_{10}H_{16})Cl_2(pyridine)]$[46] was chosen as a reference compound for a monomer complex because it is unable to form intermolecular hydrogen bonds. The comparison was carried out between DOSY experiments from two different but equally prepared NMR samples of complex **3** and the ruthenium pyridine complex, respectively, to avoid interactions between the two compounds in a mixed sample. The measured diffusion coefficient for complex **3** ($D = 1.17 \times 10^{-9}$ m^2 s^{-1}; log $D = -8.93$) is smaller that measured for the pyridine complex ($D = 1.44 \times 10^{-9}$ m^2 s^{-1}; log $D = -8.84$),[47] denoting a larger molecule in solution than the pyridine complex. The expected ratio between the diffusion coefficients of two spherical molecules, one having twice the volume of the other, is 1.26: $(MW_b/MW_a)^{1/3} = (2)^{1/3} = 1.26 = D_a/D_b$. In this case, the ratio between the diffusion coefficients of the complex **3** and that of the pyridine complex ($D_{[Ru]-Py}/D_3 = 1.23$) estimates for complex **3** an intermediate molecular weight between the monomer and that expected for a dimer complex formed by the hydrogen-bond union of two monomers. This result accounts for an equilibrium situation in solution between monomer and dimer species, so an average diffusion coefficient pondered by the extension of this dynamic process is measured.

Additional DOSY experiments were carried out in order to gain more insight into this proposed intermolecular equilibrium. Thus, several ^{1}H DOSY experiments were performed on a 24 mM sample of complex **3** in CD_2Cl_2 by varying the diffusion time (50, 100, 200, 300, and 500 ms) of each measurement to detect any dynamic process or exchange phenomenon occurring in the molecule.[43b] The DOSY plots showed some differences between the diffusion coefficients exhibited by the different protons in the molecule (see Table 4). The CH resonances afforded a diffusion coefficient $D = 1.17 \times 10^{-9}$ m^2 s^{-1} (log $D = -8.93$) in all of the experiments with different diffusion times; the diffusion coefficient for the NH-2 proton at 11.74 ppm was slightly displaced, $D = 1.20 \times 10^{-9}$ m^2 s^{-1} (log $D = -8.92$), but also independent of the diffusion time; however, the diffusion coefficient displayed by the NH-4 proton at 9.10 ppm was a bit larger than the coefficient of the other protons in all of the measurements, and on the other hand, its value became larger

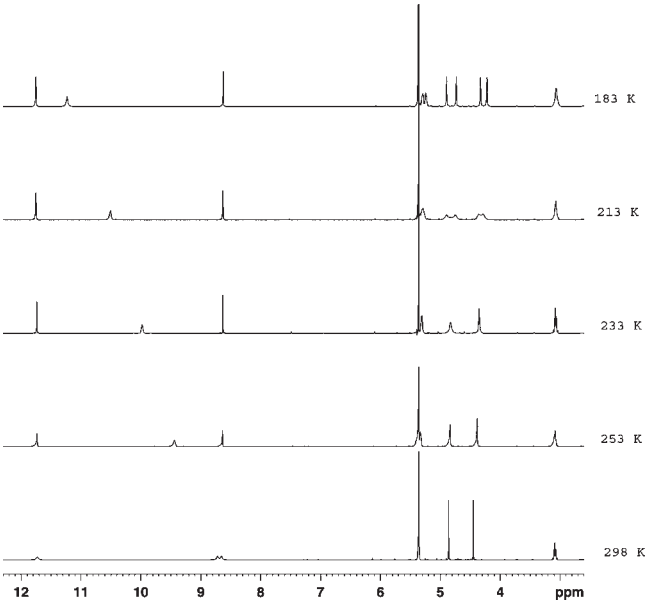

Figure 13. Details of the variable-temperature ^{1}H NMR experiments for complex **3** (CD_2Cl_2).

($D = 1.29-1.58$; log $D = -8.89$ to -8.80) with increasing diffusion times.

The diffusing behavior of the NH-4 proton represents the exchange of this labile proton with residual water in the deuterated solvent, as has been previously reported for similar uracile free molecules.[48] On the other hand, poorly resolved signals in the indirect dimension for the allylic terminal protons may be indicative of the presence of a dynamic process not detected in the time scale of these DOSY experiments.

An additional proof for the presence of intermolecular hydrogen bonds was obtained when the DOSY experiments were performed on more diluted NMR samples of complex **3** (18, 12, and 5 mM) with the same diffusion time (D20 = 120 ms). The diffusion coefficient displayed by all of the protons in the molecule increased with dilution: $D = 1.17-1.35$ (log $D = -8.93$ to -8.87) for the CH protons and $D = 1.32-1.58$ (log $D = -8.88$ to -8.80) for the NH-4 protons. In Figure 14, expansions of the DOSY spectra of the 24 and 5 mM samples are compared. This result is in good agreement with a larger presence of monomer species in diluted solutions.

dx.doi.org/10.1021/ic200547k |Inorg. Chem. 2011, 50, 4868–4881

Table 4. Diffusion Coefficient D ($\times 10^{-9}$ m^2 s^{-1}) [a] of Complex 3

	diffusion time (D20, ms) in a 24 mM NMR sample					concentration of the NMR sample (mM) for a diffusion time D20 = 120 ms			
	50	100	200	300	500	24	18	12	5
CH	1.17	1.17	1.17	1.17	1.17	1.17	1.29	1.32	1.35
NH-2	1.20	1.20	1.20	1.20	1.20	1.20	1.38	1.38	1.38
NH-4	1.29	1.32	1.38	1.44	1.58	1.32	1.41	1.48	1.58

[a] The DOSY experiments were acquired with the bipolar longitudinal eddy current delay pulse program with spinning of the sample to avoid convection influence. See the Experimental Section for details.

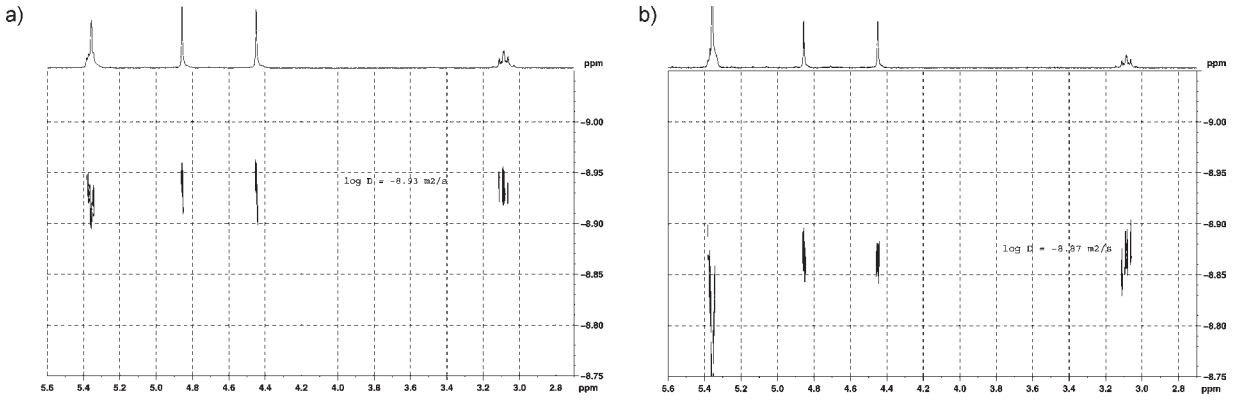

Figure 14. (a) Details of the DOSY spectrum of a 24 mM NMR sample of complex **3** in CD_2Cl_2. (b) Details of the DOSY spectrum of a 5 mM NMR sample of complex **3** in CD_2Cl_2.

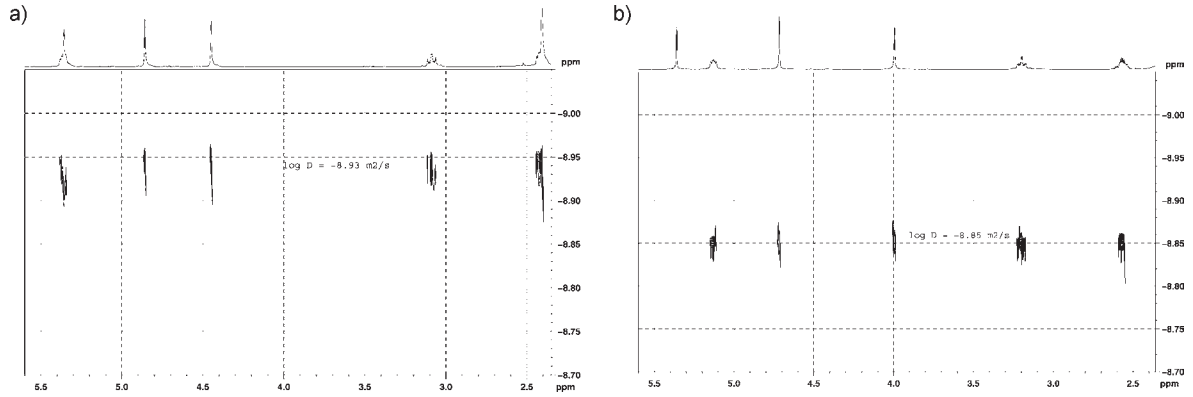

Figure 15. (a) Details of the DOSY spectrum of complex **3** in CD_2Cl_2 without DMSO. (b) Details of the DOSY spectrum of complex **3** in CD_2Cl_2 with DMSO.

Taking advantage of the known tendency of dimethyl sulfoxide (DMSO) to break up hydrogen bonds,[42a] a limit situation in which only monomer molecules would be present was forced by adding a drop of DMSO-d_6 to an NMR sample of complex **3** in CD_2Cl_2. As depicted in Figure 15, the new measured diffusion coefficient was larger that obtained without DMSO. The CH and NH-2 protons afforded a diffusion coefficient $D = 1.41 \times 10^{-9}$ m^2 s^{-1} (log $D = -8.85$), whereas the coefficient exhibited by the NH-4 proton was a bit larger, $D = 1.51 \times 10^{-9}$ m^2 s^{-1} (log $D = -8.82$). When compared with the diffusion coefficient of the reference ruthenium−pyridine complex ($D_{[Ru]-Py}/D_{3\text{-DMSO}} = 1.44/1.41 = 1.023$), the new diffusion coefficient measured in the presence of DMSO would fit the expected value for a monomeric species of complex **3**.

Also, in the new ^{1}H NMR spectrum at 298 K, it is noticeable that the chemical shift for the NH-4 proton has been shifted from 9.10 to 11.23 ppm, indicating that this NH proton is now solvated by DMSO molecules, preventing its participation in intermolecular hydrogen bonds, while the signal for the NH-2 proton remains at 11.75 ppm. However, when variable-temperature ^{1}H NMR experiments were recorded, it was observed that both signals shifted to lower fields when the temperature was lowered, showing the typical behavior of labile protons and therefore providing proof that the addition of DMSO-d_6 has also broken the intramolecular hydrogen bond between the NH-2 proton and the chlorine ligands. Accordingly, from 298 to 183 K, no splitting of the signals is found, indicating equivalent environments for the halves of 2,7-dimethyloctadienediyl in the

dx.doi.org/10.1021/ic200547k |Inorg. Chem. 2011, 50, 4868–4881

Table 5. Complex 3 Catalyzed Isomerization of 1-Octen-3-ol into Octan-3-one [a]

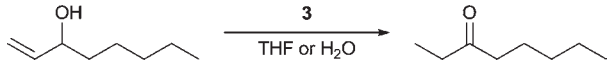

entry	solvent	T (°C)	mol % 3	mol % KO^{t}Bu	time	yield (%)[b]	TOF (h^{-1})[c]
1	THF	75	0.2		24 h	99	21
2	THF	75	0.2	0.4	40 min	99	743
3	H_2O	75	0.2		10 min	99	2970
4	H_2O	35	1		3 h	99	33

[a] Reactions performed under a nitrogen atmosphere using 1 mmol of 1-octen-3-ol (0.2 M). [b] Yield of octan-3-one determined by gas chromatography. [c] Turnover frequencies [(mol of product/mol of ruthenium)/time] were calculated at the time indicated in each case.

range of temperatures and denoting a free rotation about the Ru−N bond.

In conclusion, NMR characterization and diffusion studies have proven the existence of intramolecular hydrogen bonds for complex **3** in a poorly coordinating solvent (CD_2Cl_2). The ability of the uracil moiety to establish also intermolecular hydrogen bonds leads to an equilibrium between monomer and dimer species in solution whose extension depends on the temperature, concentration, and coordinating properties of the solvent, and therefore the equilibrium situation can be modulated by varying the reaction conditions.

Catalytic Studies. Because it is presently well documented that inter- and intramolecular hydrogen bonding are playing a role in the activity of bifunctional catalysts,[6,7] we believed it of interest to check whether the existence of these types of interactions in the above-described complexes would affect their catalytic activities. Following our previous catalytic studies on the isomerization of allylic alcohols catalyzed by ruthenium(IV) complexes, isomerization of the allylic alcohol 1-octen-3-ol into octan-3-one was tested using complex **3** as a reference case (Table 5). In a model reaction, when a 0.2 M tetrahydrofuran (THF) solution of 1-octen-3-ol was refluxed for 24 h with a catalytic amount of **3** (0.2 mol %), a quantitative yield of octan-3-one was obtained (entry 1). Although complex **3** is active in the absence of a base as the cocatalyst, a higher activity is achieved in the presence of 0.4 mol % KO^{t}Bu, reaching a quantitative conversion in ca. 40 min (TOF = 743 h^{-1}, entry 2). This turnover (TOF) value can be compared to those shown by analogous mononuclear ruthenium(IV) catalysts, i.e., [Ru(η^3:η^3-$C_{10}H_{16}$)Cl_2(P^{i}Pr$_3$)] (TOF = 750 h^{-1}) and [Ru(η^3:η^3-$C_{10}H_{16}$)Cl_2(NH_2Ph)] (TOF = 500 h^{-1}).[13d] Taking advantage of the solubility of complex **3** in water, we decided to perform the catalytic study in an aqueous medium. Remarkably, the reaction proceeds at a higher rate than those observed for THF even in the absence of a base, reaching a quantitative conversion into octan-3-one in only 10 min versus 24 h in THF. It is also worth mentioning that the exceptional catalytic activity of complex **3** is maintained at room temperature (entry 4; 99%; 3 h), a catalytic performance reported for only a limited number of metal catalysts in water.[49] Although no mechanistic studies have been carried out, this enhanced catalytic activity is probably related with both the presence of hydrogen bonding arising from both the N−H and C═O groups of the uracile ligand and the formation of the aqua complexes as intermediate active species. These facts enable the ability of complex **3** to act as a bifunctional catalyst, favoring interaction with the allylic alcohol.

CONCLUSIONS

Here we describe novel ruthenium(IV) complexes bearing two-electron N-heterocyclic ligands such as pyrazole derivatives (**2b**−**2e**), 6-azauracil (**3**), and 1*H*-indazol-3-ol (**4**). The presence of uncoordinated C═O, N−H, and O−H groups in these ligands prone to form hydrogen bonds provides the appearance in the new complexes of intra- and intermolecular hydrogen interactions. Several ruthenium(IV) complexes of this type have been characterized by X-ray diffraction in the solid state, showing the nature of hydrogen bonding of the following type: (a) intramolecular ones between pyrazole or indazole N−H and chloride ligands; (b) intermolecular ones through N−H or O−H and chloride ligands featuring large molecular arrays. The packing diagram of the 2-(1*H*-pyrazol-3-yl)phenol complex **2e** is significant in the series (Figure 11) because shows the ability of the pyrazole N−H and chloride ligands to participate in hydrogen bonding with the O−H not only intramolecular but also intermolecular with the O−H of a neighboring molecule in the crystal. This pattern of hydrogen interaction may model those featured by a pyrazole bifunctional catalyst either with hydroxylic solvents including water or for the activation of analogous protic substrates.

The existence of intermolecular hydrogen bonds has also been investigated in solution by means of NMR diffusion studies in the uracil complex **3**. Complex **3** is a dimer in the solid state based on relatively short intermolecular N−H···O hydrogen bonds (2.00 Å). DOSY experiments show that the ability of the N−H and C═O groups to form intermolecular hydrogen bonds leads to an equilibrium between monomer and dimer species in solution whose extension depends on the temperature, concentration, and coordinating properties of the solvent. Finally, it is worth mentioning that preliminary studies have shown that complex **3** containing the uracil ligand able to form intra- and intermolecular hydrogen bonding is a highly efficient catalyst for redox isomerization of 1-octen-3-ol into octan-3-one, a catalytic activity that is among the most efficient reported to date. Further experimental and theoretical work on the catalytic activity of these types of complexes for the redox isomerization of allylic alcohols in water focused on exploring the influence of hydrogen bonding will be published elsewhere.

ASSOCIATED CONTENT

Supporting Information. Cartesian coordinates and total electronic energies for the computed species **J** and **K** and an X-ray crystallographic file in CIF format. This material is available free of charge via the Internet at http://pubs.acs.org.

AUTHOR INFORMATION

Corresponding Author

*E-mail: jgh@uniovi.es (J.G.), erubio@uniovi.es (E.R.).

ACKNOWLEDGMENT

Financial support from the Spanish MICINN (Projects CTQ2006-08485/BQU, CTQ2010-14796/BQU, Consolider Ingenio CSD2007-00006, and CTQ2007-61048) and Gobierno

del Principado de Asturias (FICYT Project IB08-036) is acknowledged.

REFERENCES

(1) (a) Jeffrey, G. A.; Saenger, W. *Hydrogen Bond in Biological Structures*; Springer: Berlin, 1991. (b) Jeffrey, G. A. *Introduction to Hydrogen Bonding*; Oxford University Press: Oxford, U.K., 1997. (c) Scheiner, S. *Hydrogen Bonding: A Theoretical Perspective*; Oxford University Press: Oxford, U.K., 1997. (d) Desiraju, G. R.; Steiner, T. *The Weak Hydrogen Bond in Structural Chemistry and Biology*; Oxford University Press: Oxford, U.K., 1999.

(2) For leading reviews, see: (a) Taylor, M. S.; Jacobsen, E. N. *Angew. Chem., Int. Ed.* **2006**, *45*, 1520. (b) Prins, L. J.; Reinhoudt, D. N.; Timmerman, P. *Angew. Chem., Int. Ed.* **2001**, *40*, 2382. (c) Schneiner, P. R. *Chem. Soc. Rev.* **2003**, *32*, 289. (d) Zhang, Z. G.; Schneiner, P. R. *Chem. Soc. Rev.* **2009**, *38*, 11878. (e) Yu, X. H.; Wang, W. *Chem.—Asian J.* **2008**, *3*, 516.

(3) (a) Fontecilla-Camps, J. C. In *Bioorganometallics*; Jaouen, G. Ed.; Wiley-VCH: Weinheim, Germany, 2006; p 353. (b) Frausto da Silva, J. J. R.; Williams, R. J. P. *The Biological Chemistry of the Elements*, 2nd ed.; Oxford University Press: Oxford, U.K., 2001. (c) Stryer, L. *Biochemistry*, 5th ed.; Freeman: New York, 2002. (d) Borovik, A. S. *Acc. Chem. Res.* **2005**, *38*, 54. (e) Holm, R. H.; Solomon, E. L. *Chem. Rev.* **1996**, *96*; *Chem. Rev.* **2004**, 104.

(4) (a) Crabtree, R. B.; Siegbahn, P. E. M.; Eisenstein, O.; Rheingold, A. L.; Koetzle, T. F. *Acc. Chem. Res.* **1996**, *29*, 348. (b) Epstein, L. M.; Shubina, E. S. *Coord. Chem. Rev.* **2002**, *231*, 165. (c) Brammer, L. *Dalton Trans.* **2003**, 3145.

(5) Natale, D.; Mareque-Rivas, J. C. *Chem. Commun.* **2008**, 425.

(6) For leading accounts on bifunctional organometallic catalysts, see: (a) Grotjahn, D. B. *Dalton Trans.* **2008**, 6497. (b) Grotjahn, D. B. *Chem. Lett.* **2010**, *39*, 908. (c) Grotjahn, D. B. *Chem.—Eur. J.* **2005**, *11*, 7146. (d) Saburi, H.; Tanaka, S.; Kitamura, M. *Angew. Chem., Int. Ed.* **2005**, *44*, 1730. (e) Ikariya, T.; Muratta, K.; Noyori, R. *Org. Biomol. Chem.* **2006**, *4*, 393. (f) Ikariya, T.; Blacker, J. *Acc. Chem. Res.* **2007**, *40*, 1300. (g) Ikariya, T.; Gridnev, I. D. *Top. Catal.* **2010**, *53*, 894.

(7) (a) Yamakava, M.; Ito, H.; Noyori, R. *J. Am. Chem. Soc.* **2000**, *122*, 1466. (b) Shvo, Y.; Czarkie, D.; Rahamin, Y. K. *J. Am. Chem. Soc.* **1986**, *108*, 7400. (c) Casey, C. P.; Johnson, J. B. *J. Org. Chem.* **2003**, *68*, 1998. (d) Casey, C. P.; Singer, S. W.; Powell, D. R.; Hayashi, R. K.; Kavan, M. *J. Am. Chem. Soc.* **2001**, *123*, 1090. For mechanistic calculations, see: (e) Comas-Vives, A.; Ujaque, G.; Lledós, A. *Organometallics* **2007**, *26*, 4135. (f) Handgraaf, J.-W.; Meijer, E. V. *J. Am. Chem. Soc.* **2007**, *129*, 3099. (g) Casey, C. P.; Bikzhanova, G. A.; Cui, Q.; Guzei, I. A. *J. Am. Chem. Soc.* **2005**, *127*, 14062. For other analogous examples, see: (h) Hayashi, T.; Kawamura, N.; Ito, Y. *J. Am. Chem. Soc.* **1987**, *109*, 7876. (i) Ito, M.; Kitahara, S.; Ikariya, T. *J. Am. Chem. Soc.* **2005**, *127*, 6172. (j) Zweifel, T.; Naubron, J.-V.; Bütner, T.; Ott, T.; Grützmacher, H. *Angew. Chem., Int. Ed.* **2008**, *47*, 3245. (k) Johnson, J. B.; Bäckwall, J. E. *J. Org. Chem.* **2003**, *68*, 7681. For a review, see: (l) Ikariya, T.; Gridnev, I. D. *Top. Catal.* **2010**, *53*, 894.

(8) Intramolecular ligand−ligand interactions through hydrogen bonding in catalytic processes have also been reported: (a) Breit, B. *Angew. Chem., Int. Ed.* **2005**, *44*, 6816. (b) Smejkal, T.; Breit, B. *Angew. Chem., Int. Ed.* **2008**, *47*, 311. (c) de Greef, M.; Breit, B. *Angew. Chem., Int. Ed.* **2009**, *48*, 551. (d) Breit, B.; Seiche, W. *Angew. Chem., Int. Ed.* **2005**, *44*, 1640. (e) Breit, B.; Seiche, W. *J. Am. Chem. Soc.* **2003**, *125*, 6608. (f) Gellrich, U.; Huang, J.; Seiche, W.; Keller, M.; Meuwly, M.; Breit, B. *J. Am. Chem. Soc.* **2011**, *133*, 964.

(9) Hydrogen interactions also play an important role in the number of stoichiometric C−H activation reactions. For instance, see: (a) Grotjahn, D. B.; Kragulj, E. J.; Zeinalipour-Yazdi, C. D.; Miranda-Soto, V.; Lev, D. A.; Coosksy, A. L. *J. Am. Chem. Soc.* **2008**, *130*, 10860. (b) Grotjahn, D. B.; Miranda-Soto, V.; Kragulj, E. J.; Lev, D. A.; Erdogan, G.; Zeng, X.; Coosksy, A. L. *J. Am. Chem. Soc.* **2008**, *130*, 20. (c) Conejero, S.; Lara, P.; Paneque, M.; Petronilho, A.; Poveda, M. L.; Serrano, O.; Vattier, F.; Álvarez, E.; Maya, C.; Salazar, V.; Carmona, E. *Angew. Chem., Int. Ed.* **2008**, *47*, 4380. (d) Álvarez, E.; Hernandez, Y. A.; López-Serrano, J.; Maya, C.; Paneque, M.; Petronilho, A.; Poveda, M. L.; Salazar, V.; Vattier, F.; Carmona, E. *Angew. Chem., Int. Ed.* **2010**, *49*, 3496.

(10) (a) Chevalier, F.; Breit, B. *Angew. Chem., Int. Ed* **2006**, *45*, 1599. Anti-Markovnikov regioselective hydration of alkynes to aldehydes showing an acceleration rate of 2×10^{11} fold over the noncatalyzed reaction has been reported: (b) Grotjahn, D. B.; Incarvito, C. D.; Rheingold, A. L. *Angew. Chem., Int. Ed.* **2001**, *40*, 3884. (c) Grotjahn, D. B.; Lev, D. A. *J. Am. Chem. Soc.* **2004**, *126*, 12232. (d) Nair, R. N.; Lee, P. J.; Rheingold, A. J.; Grotjahn, D. B. *Chem.—Eur. J.* **2010**, *16*, 7992.

(11) Hydrogen interactions have been proposed as being responsible for the enhanced rate observed in the hydration of nitriles catalyzed by ruthenium complexes: (a) Fung, W. K.; Huang, X.; Man, M. L.; Ng, S. M.; Hung, M. Y.; Lin, Z. *J. Am. Chem. Soc.* **2003**, *125*, 11539. (b) Smejkal, T.; Breit, B. *Organometallics* **2007**, *26*, 2461. (c) Chevalier, F.; Breit, B. *Angew. Chem., Int. Ed.* **2006**, *45*, 1599. (d) Chevalier, F.; Breit, B. *Angew. Chem.* **2006**, *118*, 1629. (e) Cadierno, V.; Francos, J.; Gimeno, J. *Chem.—Eur. J.* **2008**, *14*, 6601. (f) Cadierno, V.; Díez, J.; Francos, J.; Gimeno, J. *Chem.—Eur. J.* **2010**, *16*, 9808.

(12) An elegant case consisting of a five-coordinated aquoiridium(I) complex shows that water has a strong influence on the stoichiometric regioselective α-CH sp^3 activation of ketones via stabilization of the metalated product by hydrogen bonding of the carbonyl group with the coordinated water molecule. Feller, M.; Karton, A.; Leitus, G.; Martin, J. M. L.; Milstein, D. *J. Am. Chem. Soc.* **2006**, *128*, 12400.

(13) (a) Cadierno, V.; García-Garrido, S. E.; Gimeno, J. *Chem. Commun.* **2004**, 232. (b) Cadierno, V.; Crochet, P.; García-Garrido, S. E.; Gimeno, J. *Dalton Trans.* **2004**, 3635. (c) Cadierno, V.; García-Garrido, S. E.; Gimeno, J.; Nebra, N. *Chem. Commun.* **2005**, 4086. (d) Cadierno, V.; García-Garrido, S. E.; Gimeno, J.; Varela-Álvarez, A.; Sordo, J. A. *J. Am. Chem. Soc.* **2006**, *128*, 1360. (e) Crochet, P.; Díez, J.; Fernández-Zúmel, M. A.; Gimeno, J. *Adv. Synth. Catal.* **2006**, *348*, 93. (f) Díaz-Álvarez, A. E.; Crochet, P.; Zablocka, M.; Duhayon, C.; Cadierno, V.; Gimeno, J.; Majoral, J. P. *Adv. Synth. Catal.* **2006**, *348*, 1671. (g) Cadierno, V.; García-Garrido, S. E.; Gimeno, J. *J. Am. Chem. Soc.* **2006**, *128*, 15094. (h) Cadierno, V.; Francos, J.; Gimeno, J.; Nebra, N. *Chem. Commun.* **2007**, 2536. (i) Cadierno, V.; Gimeno, J.; Nebra, N. *Chem.—Eur. J.* **2007**, *13*, 6590. (j) Díaz-Álvarez, A. E.; Crochet, P.; Zablocka, M.; Duhayon, C.; Cadierno, V.; Majoral, J.-P. *Eur. J. Inorg. Chem.* **2008**, 786. (k) Cadierno, V.; Crochet, P.; Gimeno, J. *Synlett* **2008**, 1105. (l) Cadierno, V.; Crochet, P.; Francos, J.; García-Garrido, S. E.; Gimeno, J.; Nebra, N. *Green Chem.* **2009**, *11*, 1992. (m) Cadierno, V.; Francos, J.; Gimeno, J. *Green Chem.* **2010**, *12*, 135. (n) Cadierno, V.; Francos, J.; Gimeno, J. *Chem. Commun.* **2010**, *46*, 4175. (o) Lastra-Barreira, B.; Díez, J.; Crochet, P. *Green Chem.* **2009**, *11*, 1681.

(14) (a) Porri, L.; Gallazzi, M. C.; Colombo, A.; Allegra, G. *Tetrahedron Lett.* **1965**, *47*, 4187. (b) Salzer, A.; Bauer, A.; Podewils, F. In *Synthetic Methods of Organometallic and Inorganic Chemistry*; Herrmann, W. A., Ed.; Thieme Verlag: Stuttgart, Germany, 2000; Vol. 9, p 36. (c) Salzer, A.; Bauer, A.; Geyser, S.; Podewils, F.; Turpin, G. C.; Ernst, R. D. *Inorg. Synth.* **2004**, *34*, 59.

(15) (a) Toerien, J. G.; van Rooyen, P. H. *J. Chem. Soc., Dalton Trans.* **1991**, 1563. (b) Steed, J. W; Tocher, D. A. *J. Chem. Soc., Dalton Trans.* **1992**, 2765.

(16) *CrysAlis^{Pro} CCD* and *CrysAlis^{Pro} RED*; Oxford Diffraction Ltd.: Abingdon, Oxfordshire, U.K., 2008.

(17) *Bruker: Collect data collection software*; Bruker AXS: Delft, The Netherlands, 2004.

(18) Otwinowski, Z.; Minor, W. *Methods Enzymol.* **1997**, *276*, 307.

(19) Blessing, R. H. *Acta Crystallogr.* **1995**, *A51*, 33.

(20) Farrugia, L. J. *J. Appl. Crystallogr.* **1999**, *32*, 837.

(21) Beurskens, P. T.; Admiraal, G.; Beurskens, G.; Bosman, W. P.; García-Granda, S.; Gould, R. O.; Smits, J. M. M.; Smykalla, C. *The DIRDIF Program System*; Technical Report of the Crystallographic Laboratory, University of Nijmegen: Nijmegen, The Netherlands, 1999.

(22) Altomara, A.; Cascarano, G.; Giacovazzo, C.; Gualardi, A. *J. Appl. Crystallogr.* **1993**, *26*, 343.

(23) Sheldrick, G. M. *SHELXL97: Program for the Refinement of Crystal Structures*; University of Göttingen: Göttingen, Germany, 1997.
(24) *Tables for X-Ray Crystallography*; Kynoch Press: Birminghan, U.K., 1974; Vol. *IV* (present distributor: Kluwer Academic Publishers: Dordrecht, The Netherlands).
(25) Nardelli, M. *Comput. Chem.* **1983**, *7*, 95.
(26) Spek, A. L. *PLATON: A Multipurpose Crystallographic Tool*; University of Utrecht: Utrecht, The Netherlands, 2007.
(27) *ORTEP-3 for Windows*: Farrugia, L. J. *J. Appl. Crystallogr.* **1997**, *30*, 565.
(28) Frisch, M. J.; Trucks, G. W.; Schlegel, H. B.; Scuseria, G. E.; Robb, M. A.; Cheeseman, J. R.; Montgomery, J. A., Jr.; Vreven, T.; Kudin, K. N.; Burant, J. C.; Millam, J. M.; Iyengar, S. S.; Tomasi, J.; Barone, V.; Mennucci, B.; Cossi, M.; Scalmani, G.; Rega, N.; Petersson, G. A.; Nakatsuji, H.; Hada, M.; Ehara, M.; Toyota, K.; Fukuda, R.; Hasegawa, J.; Ishida, M.; Nakajima, T.; Honda, Y.; Kitao, O.; Nakai, H.; Klene, M.; Li, X.; Knox, J. E.; Hratchian, H. P.; Cross, J. B.; Adamo, C.; Jaramillo, J.; Gomperts, R.; Stratmann, R. E.; Yazyev, O.; Austin, A. J.; Cammi, R.; Pomelli, C.; Ochterski, J. W.; Ayala, P. Y.; Morokuma, K.; Voth, G. A.; Salvador, P.; Dannenberg, J. J.; Zakrzewski, V. G.; Dapprich, S.; Daniels, A. D.; Strain, M. C.; Farkas, O.; Malick, D. K.; Rabuck, A. D.; Raghavachari, K.; Foresman, J. B.; Ortiz, J. V.; Cui, Q.; Baboul, A. G.; Clifford, S.; Cioslowski, J.; Stefanov, B. B.; Liu, G.; Liashenko, A.; Piskorz, P.; Komaromi, I.; Martin, R. L.; Fox, D. J.; Keith, T.; Al-Laham, M. A.; Peng, C. Y.; Nanayakkara, A.; Challacombe, M.; Gill, P. M. W.; Johnson, B.; Chen, W.; Wong, M. W.; Gonzalez, C.; Pople, J. A. *Gaussian 03*, revision C.02; Gaussian, Inc.: Wallingford, CT, 2004.
(29) (a) Becke, A. D. *J. Chem. Phys.* **1993**, *98*, 5648. (b) Lee, C.; Yang, W.; Parr, R. G. *Phys. Rev. B* **1988**, *37*, 785. (c) Stephens, P. J.; Devlin, F. J.; Chabalowski, C. F.; Frisch, M. J. *J. Phys. Chem.* **1994**, *98*, 11623.
(30) (a) Hay, P.; Wadt, W. R. *J. Chem. Phys.* **1985**, *82*, 270. (b) Wadt, W. R.; Hay, P. *J. Chem. Phys.* **1985**, *82*, 284. (c) Hay, P.; Wadt, W. R. *J. Chem. Phys.* **1985**, *82*, 299.
(31) (a) Barone, V.; Cossi, M. *J. Phys. Chem. A* **1998**, *102*, 1995. (b) Cossi, M.; Rega, N.; Scalmani, G.; Barone, V. *J. Comput. Chem.* **2003**, *24*, 669.
(32) Esturau, N.; Sánchez-Ferrando, F.; Gavín, J. A.; Roumestand, C.; Delsuc, M.-A.; Parella, T. *J. Magn. Reson.* **2001**, *153*, 48.
(33) Available from Strem Chemicals, Inc., since 2006 (catalog no. 44-0203).
(34) For a general review on the coordination chemistry and catalytic applications of complex **1**, see: Cadierno, V.; Crochet, P.; García-Garrido, S. E.; Gimeno, J. *Curr. Org. Chem.* **2006**, *10*, 165.
(35) Cornago, P.; Cabildo, P.; Claramunt, R. M.; Bouissane, L.; Pinilla, E.; Torres, M. R.; Elguero, J. *New J. Chem.* **2009**, *33*, 125.Claramunt, R. M.; García, M. A.; López, C.; Trofimenko, S.; Yap, G. P. A.; Alkorta, I.; Elguero, J. *Magn. Reson. Chem.* **2005**, *43*, 89 and references cited therein.
(36) (a) Gupta, R. K.; Singh, A. K.; Yadav, M.; Kumar, P.; Singh, S. K.; Li, P.; Xu, Q.; Pandey, D. S. *J. Organomet. Chem.* **2010**, *695*, 1924. (b) Kollipara, M. R. *J. Organomet. Chem.* **2004**, *689*, 3265 and references cited therein.
(37) (a) Mishra, H.; Mukherjee, R. *J. Organomet. Chem.* **2007**, *692*, 3248. (b) Fijita, H.; Uchida, T.; Irie, R.; Katsuki, T. *Chem. Lett.* **2007**, *36*, 1092.
(38) For other intramolecular hydrogen bonding between halide and pyrazol ligands, see: (a) Reedijk, J.; Stork-Blaisse, B. A.; Versschoor, G. C. *Inorg. Chem.* **1971**, *10*, 2594. (b) Mighell, A. D.; Reimann, C. V.; Santoro, A. *Acta Crystallogr., Sect. B* **1969**, *B25*, 595. (c) Reimann, C. V. *J. Chem. Soc., Chem. Commun.* **1969**, 145. (d) Reimann, C. V.; Mighell, A. D.; Mauer, F. A. *Acta Crystallogr.* **1967**, *23*, 135. (e) Esteruelas, M. A.; Oliván, M.; Oñate, E.; Ruiz, N.; Tejada, M. A. *Organometallics* **1999**, *18*, 2953.
(39) Steiner, T. *Angew. Chem., In. Ed.* **2002**, *41*, 48.
(40) A similar intramolecular hydrogen bond has also been claimed as responsible for the high chemical shift (13.6−13.9 ppm) of the SH protons in other ruthenium(IV) complexes with 2,7-dimethyloctadiene-diyl- and thiol-containing ligands.[15a]
(41) (a) Johnson, C. S., Jr. *Prog. Nucl. Magn. Reson. Spectrosc.* **1999**, *34*, 203. (b) Morris, K. F.; Johnson, C. S., Jr. *J. Am. Chem. Soc.* **1992**, *114*, 3139.
(42) (a) Kapur, G. S.; Cabrita, E. J.; Berger, S. *Tetrahedron Lett.* **2000**, *41*, 7181. (b) Cabrita, E. J.; Berger, S. *Magn. Reson. Chem.* **2001**, *39*, S142. (c) de Carvalho, E. M.; Velloso, M. H. R.; Tinoco, L. W.; Figueroa-Villar, J. D. *J. Magn. Reson.* **2003**, *164*, 197. (d) Brand, T.; Cabrita, E. J.; Berger, S. *Prog. Nucl. Magn. Reson. Spectrosc.* **2005**, *46*, 159.
(43) (a) Cabrita, E. J.; Berger, S.; Bräuer, P.; Kärger, J. *J. Magn. Reson.* **2002**, *157*, 124. (b) Cabrita, E. J.; Berger, S. *Magn. Reson. Chem.* **2002**, *40*, S122.
(44) Stokes−Einstein equation: $D = K_BT/6\pi\eta r_H$, where D = diffusion coefficient, K_B = Boltzmann's constant, η = solvent viscosity, and r_H = hydrodynamic radius.
(45) (a) Valentini, M.; Pregosin, P. S.; Rüegger, H. *J. Chem. Soc., Dalton Trans.* **2000**, 4507. (b) Crutchfield, C. A.; Harris, D. J. *J. Magn. Reson.* **2007**, *185*, 179.
(46) Cox, D. N.; Roulet, R. *Inorg. Chem.* **1990**, *29*, 1360.
(47) The reported diffusion coefficients are taken from the resonance of the aliphatic CH_2 protons in both compounds.
(48) Thureau, P.; Ancian, B.; Viel, S.; Thévand, A. *Chem. Commun.* **2006**, 200.
(49) Other examples of catalytic redox isomerization of allylic alcohols in aqueous media have been reported. (a) McGrath, D. V.; Grubbs, R. H.; Ziller, J. W. *J. Am. Chem. Soc.* **1991**, *113*, 3611. (b) Karlen, T.; Ludi, A. *Helv. Chim. Acta* **1992**, *75*, 1604. (c) Bricout, H.; Monflier, E.; Carpentier, J. F.; Mortreux, A. *Eur. J. Inorg. Chem.* **1998**, 1739. (d) Schumann, H.; Ravindar, V.; Meltser, L.; Baidossi, W.; Sasson, Y.; Blum, J. *J. Mol. Catal. A* **1997**, *118*, 55. (e) de Bellefon, C.; Caravieilhes, S.; Kuntz, E. G. *C. R. Acad. Sci., Ser. IIc: Chim.* **2000**, *3*, 607. (f) Bianchini, C.; Meli, A.; Oberhauser, W. *New J. Chem.* **2001**, *25*, 11. (g) Knight, D. A.; Schull, T. L. *Synth. Commun.* **2003**, *33*, 827. (h) Crochet, P.; Fernandez-Zúmel, M. A.; Gimeno, J.; Scheele, M. *Organometallics* **2006**, *25*, 4846. (i) Campos-Malpartida, T.; Fekete, M.; Joó, F.; Kathó, A.; Romerosa, A.; Saoud, M.; Wojtków, W. *J. Organomet. Chem.* **2008**, *693*, 468. (j) Ahlsten, N.; Lundberg, H.; Martín-Matute, B. *Green Chem.* **2010**, *10*, 1628 and refs 13d−13f, 13h, 13l, and13o.